BULETINUL INSTITUTULUI POLITEHNIC DIN IAŞI

Tomul LVIII (LXII)

Fasc. 1

ŞTIINŢA ŞI INGINERIA MATERIALELOR

2012 **Editura POLITEHNIUM**

BULETINUL INSTITUTULUI POLITEHNIC DIN IAŞI
Published by the
„GHEORGHE ASACHI" TECHNICAL UNIVERSITY OF IAŞI
Editorial Office: Bd. D. Mangeron 63, 700050, Iaşi, ROMANIA
Tel. 40-232-278683; Fax: 40-232 237666; e-mail: polytech@mail.tuiasi.ro

BULETINUL INSTITUTULUI POLITEHNIC DIN IAŞI
BULLETIN OF THE POLYTECHNIC INSTITUTE OF IAŞI
Tomul LVIII (LXII), Fasc. 1 2012

ŞTIINŢA ŞI INGINERIA MATERIALELOR

S U M A R

BULETINUL INSTITUTULUI POLITEHNIC DIN IAŞI
BULLETIN OF THE POLYTECHNIC INSTITUTE OF IAŞI
Tomul LVIII (LXII), Fasc.1 2012

MATERIALS SCIENCE AND ENGINEERING

CONTENTS

BULETINUL INSTITUTULUI POLITEHNIC DIN IAȘI
Publicat de
Universitatea Tehnică „Gheorghe Asachi” din Iaşi
Tomul LVIII (LXII), Fasc. 1, 2012
Secția
ŞTIINŢA ŞI INGINERIA MATERIALELOR

MORPHOLOGIC CHARACTERISATION OF SOME THIN ZINC PHOSPHATE LAYERS

BY

ANDREI VICTOR SANDU*, COSTICĂ BEJINARIU, IOAN GABRIEL SANDU and CONSTANTIN BACIU

“Gheorghe Asachi” Technical University of Iaşi
Faculty of Material Science and Engineering

Received: February 28, 2012
Accepted for publication: March 7, 2012

Abstract: The paper presents the surface morphologic characterization of some thin phosphate layers on iron support. In study were involved SEM and 3D optical profilometry in order to evaluate the compactness and uniformity of the layers which are directly connected to the corrosion resistance of the samples.

Keywords: zinc phosphate layers; SEM; profilometry; particle size.

1. Introduction

As surface treatment on iron substrates, Zn phosphating is one of the most widely used. Acid aqueous phosphate solutions containing zinc ions and phosphoric acid are used (Amirudin & Thierry, 1996; Ghali & Potvin, 1972; Rausch 1990). The phosphate coating develops via the nucleation, growth, and coalescence of zinc phosphate grains. The corrosion resistance of the phosphate coating is related to the size and population density of pores in the coating; that

* Corresponding author: *e-mail*: andrew_viktor@yahoo.com

is, the pores provide a path for corrosion attack (Banczek *et al*., 2009; Flis *et al*., 1997; Zimmermann *et al*., 2003). In the anodic area Fe^{2+} ions are formed (from the support) and contribute to the formation the primary layer of zinc pyrophosphate, the resulted crystalline structures becoming inert to oxidative processes (Bejinariu *et al*., 2009; Sandu *et al*., 2010; Sandu & Bejinariu, 2010).

The article's aim is to characterize the surface morphology of the obtained zinc phosphate layers deposited on steel.

2. Materials and Methods

The sample plates (round with a diameter of 20 mm) used are mild steel DC 01 type, (SR EN 10130), used for plastic processing. Different solutions were obtained and the samples were named as following: P1, P2, P3 and P4.

First all the samples were degreased in mild alkaline bath (10 min) followed by pickling in an acid solution (20 min) and then immersion in the phosphate bath. For P1, the phosphatation solution, 1 L contains 8.2 mL H_3PO_4 98%, Zn 4g, 2.5 mL HNO_3 60%, 0.7g NaOH, 0.4g $NaNO_2$, 0.05g $Na_3P_3O_{10}$. For S2 sample was used the phosphatation solution adding 2g of hexamethylenetetramine. For S3 10 g of tannin and for S4 1 g of hexamethylenetetramine and 5 g of tannin were added. All samples were merged for 30 mins in the solutions kept at 80°C.

The researches have been carried out with a SEM VEGA II LSH scanning electron microscope manufactured by the TESCAN Co., the Czech Republic, coupled with an EDX QUANTAX QX2 detector manufactured by the BRUKER/ROENTEC Co., Germany.

For the optical profiles an 3D optical profilometer AltiSurf 500 was used. The selected areas were 2 by 2 mm.

3. Results and Discussion

In the images from Fig. 1, it can be observed the 3D surface profile of the sample surfaces, with the uniformity of the layers. Samples P1 and P3 have a very uniform structure, compared to the P2 and P4 ones.

In Fig. 2 we have the SEM images of the surface of the samples, where we can observe a clear dendritic structure for the samples P1, P2 and P3 and an non-uniformous structure on P4, where we can see also impurities.

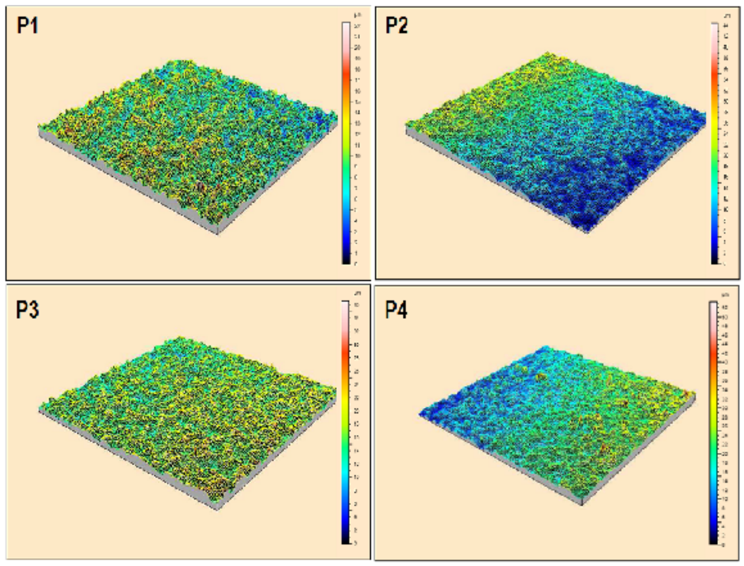

Fig. 1 – 3D Optical profiles of the samples.

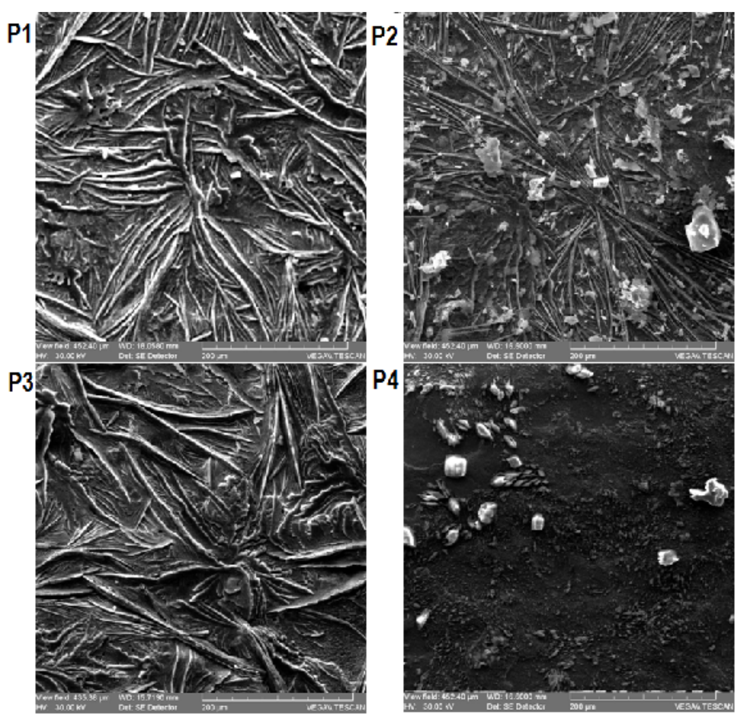

Fig. 2 – SEM images of the samples (500X).

Fig. 3 presents the particle distribution on the phosphate layers.

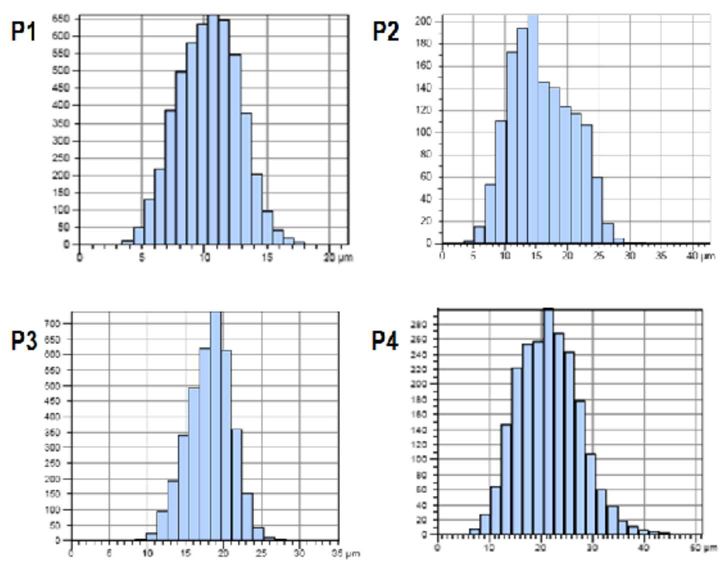

Fig. 3 – Particle Distribution (peaks/mm^2).

For sample P1 and P3 the graph has a Gaussian shape and the average dimension of the surface components is much lower and uniform. The samples P2 and P4 present particles with higher dimensions, this having a negative impact on the uniformity and compactness of the layer.

In Table 1 are shown for each sample on a surface of 4 mm^2 the number of particles, their average height and the average surface.

Table 1

Number of Particles and Their Average Height and Surface on 4 mm^2

Sample	Number of particles	Average height, [μm]	Average surface, [mm^2]
P1	517	2.17	7.7×10^{-3}
P2	340	3.09	11.8×10^{-3}
P3	450	2.41	8.8×10^{-3}
P4	400	4.81	10.1×10^{-3}

It is obvious that P1 sample has the finest and the most uniform structure, followed by P3 and P2. The P4 samples present big difference between the surface structure peaks.

3. Conclusions

From the SEM images and the 3D profilometry we can observe that sample P1 and P3 present a very compact and uniform structures, with small particles and no impurities. This causes a better corrosion resistance due to the low porosity of the layers.

The P2 sample even though presents a dendritic structure, the average size of structure components is much larger and impurities are presented on surface. P4 sample doesn't have an uniform structure, with very large particles sporadically distributed.

REFERENCES

Amirudin A., Thierry D., *Corrosion Mechanisms of Phosphated Zinc Layers on Steel as Substrates for Automotive Coatings*. Progress in Organic Coatings, **28**, 59-76, 1996.

Banczek E.P., Rodrigues P.R.P., Costa I., *Evaluation of Porosity and Discontinuities in Zinc Phosphate Coating by Means of Voltametric Anodic Dissolution (VAD)*. Surface a. Coatings Technol., **203**, 1213-1219 (2009).

Bejinariu C, Sandu I, Predescu A, Sandu IG, Baciu C, Sandu AV., *New Mechanisms for Phosphatation of Iron Objects.* Bul. Inst. Politehnic, Iaşi, s. Ştiinţa şi Ingineria Materialelor, **LV (LIX)**, *1*, 73-77 (2009).

Flis J., Tobiyama Y., Mochizuki K., Shiga C., *Characterisation of Phosphate Coatings on Zinc, Zinc–Nickel and Mild Steel by Impedance Measurements in Dilute Sodium Phosphate Solutions.* Corrosion Science, **39**, 1757-1770 (1997).

Ghali E.I., Potvin R.J.A., *The Mechanism of Phosphating of Steel*. Corrosion Science, **12**, *7*, 583-594 (1972).

Rausch W., *The Phosphating of Metals*. Finishing Publ. Ltd., UK, 406 (1990).

Sandu A.V., Bejinariu C., Predescu A., Sandu I. G., Baciu C., Sandu I., *New Mechanisms for Chemical Phosphatation of Iron Objects*. Recent Patents on Corrosion Science**, 1,** *1*, 33-37 (2011).

Sandu A.V., Bejinariu C., *Obtaining and Characterization of Superficial Phosphated Layers on Iron Support*. Bul. Inst. Politehnic, Iaşi, s. Ştiinţa şi Ingineria Materialelor, **LVI (LX)**, *2*, 113-116 (2010).

Zimmermann D., Munoz A.G., Schultze J.W.*, Microscopic Local Elements in the Phosphating Process*. Electrochimica Acta**, 48**, 3267-3277 (2003).

CARACTERIZAREA MORFOLOGICĂ A UNOR STRATURI SUBŢIRI DE FOSFAŢI DE ZINC

(Rezumat)

Se prezintă caracterizarea morfologică a suprafeţei unor straturi subţiri fosfatate pe support de fier. În studiu s-a apelat la microscopia electronică şi la profilometria optică 3D în vederea evaluării compactităţii şi uniformităţii straturilor, care sunt direct legate de rezistenţa la coroziune a probelor.

BULETINUL INSTITUTULUI POLITEHNIC DIN IAȘI
Publicat de
Universitatea Tehnică „Gheorghe Asachi” din Iaşi
Tomul LVIII (LXII), Fasc. 1, 2012
Secția
ŞTIINȚA ŞI INGINERIA MATERIALELOR

ASPECTS CONCERNING THE BIOCOMPATIBILITY OF MATERIALS USED IN DENTISTRY

BY

IRINA GRĂDINARU*, ELENA RALUCA BACIU and DANIELA CALAMAZ

"Gr. T. Popa" University of Medicine and Pharmacy of Iaşi
Faculty of Dental Medicine
Department of Dental Materials

Received: February 29, 2012
Accepted for publication: March 19, 2012

Abstract: In medicine, the biocompatibility requires an interaction between the material and the body. The placement of a restoration into the oral cavity creates an interface between the material and the tissues adjacent to the material. The interface exists, it is active and dynamic, involving two-way interactions that allow the tissue to influence the material or vice versa. In dental practice there are a number of possible biological reactions to dental materials (toxic reactions, inflammatory reactions, allergic reactions, mutagenic reactions). The use of materials to restore damaged or lost tooth structure creates specialized environments in which the biocompatibility of the material is of central importance for the long-term survival of the restoration. Three types of tests, considered basic, are used to measure the biocompatibility of the dental materials: the in vitro test, the animal test, the usage test performed either in animals or in humans. In practice, no material can be shown to be 100% safe or risk-free. The dentist must recognize that the use of materials in the oral cavity requires a risk-benefit analysis. Only the use of biocompatible materials can assure the success of the dental treatment.

Keywords: dental materials; biocompatibility; biological reactions.

* Corresponding author: *e-mail*: irigrad@yahoo.com

In medicine, the biocompatibility requires an interaction between the material and the body. Placement of a material in the body creates an interface that usually is not present. This interface that appeared is not a static one but, on the contrary, it is the site of numerous dynamic interactions between the material and the body through which the body is possible to alter the material or the material may alter the body.

The dynamics of the mentioned interactions will determine:

a) the biological response to the material;

b) the ability of the material to survive or resist degradation or corrosion in the body.

In reality, every biological interface is active, and therefore it is not possible to have a material that is inert.

The activity of this interface depends on different factors: the location of the material, the duration of the material in the body, the properties of the material and health of the host.

The placement of a restoration into the oral cavity creates an interface between the material and the tissues adjacent to the material. The interface exists, it is active and dynamic, involving two-way interactions that allow the tissue to influence the material or vice versa.

In dental practice there are a number of possible biological reactions to dental materials. These reactions have been classified classically into: toxic reactions; inflammatory reactions; allergic reactions; mutagenic reactions.

There are two important factors that appear implicated in determining the biocompatibility of a material.

The first factor involves the various types of metal corrosion / other types of material degradation. Corrosion results in the release of substances from a material into the host. The release can take many forms and may be caused by many factors. The biological response to the corrosion products depends on the amount, composition, and form of these products, as well as their location in tissues. Corrosion may be visible or invisible to the naked eye, but it is ongoing for every dental material at some level.

Corrosion is determined by the material's composition and by the biological environment in contact with the material. The biological forces that influence corrosion may be specific to an individual or they may be common to all individuals. In any case, it is the biological interface that creates the conditions for corrosion. This interface is active and dynamic, with the material affecting the body and the body affecting the material.

The second important factor which affects the biocompatibility of a material is represented by the characteristics of his surface. Research has shown for all materials that the surface of the material is quite different than its interior region. The surface is the part of a material that the body can see, the surface composition, roughness, mechanical properties, and chemical properties are critical to the biocompatibility of the material. The surface characteristics may affect the corrosion properties of a material, or they may influence biocompatibility in other ways.

The surface can also affect negatively the biological response. For numerous materials, a rough surface promotes corrosion. If the corrosion products have adverse effects, then toughness is not desirable. Roughness may also promote the adherence of bacteria and promote periodontal inflammation or teeth decay. The chemical properties of a surface may also hinder the biological response.

Several aspects of oral anatomy influence the biocompatibility of dental restorative materials. The anatomy of the tooth, the periodontal attachment, and the periapical environment has profound influences on the biological response to materials, and all are sites of interface between materials and tissues in dentistry.

The use of materials to restore damaged/lost tooth structure creates specialized environments in which the biocompatibility of the material is of central importance to the long-term survival of the dental restoration.

Three types of tests, considered basic, are used to measure the biocompatibility of the dental materials: the in vitro test; the animal test; the usage test performed either in animals or in humans.

Each test has different advantages and disadvantages; each test is used to some extent to evaluate a material before it may be sold on market. Not a single test can accurately estimate the biological response to a material and that considerable controversy exists about the appropriate mixture of the three basic types of tests.

In vitro tests, realized outside of an organism, historically, have been used as the first screening test to evaluate a new material. In vitro tests may be conducted in a test tube cell-culture dish, flask /other container, but they are performed separately from an intact organism. The material is placed into contact with some biological system (eg mammalian cells, cellular organelles, tissues, bacteria, or some sort of enzyme). The contact between material and the biological system may be direct (involves the exposure of the material directly with the biological system) or indirect (occurs through a barrier such as agar, a membrane filter / dentin).

In vitro tests can be subdivided into tests that measure cell growth or death, those that determine cellular function of some type, and those that evaluate the integrity of the genetic material of the cell.

In vitro tests have numerous advantages over animal or usage tests: are relatively fast, inexpensive, easily standardized, may be used for larger-scale screening than can either animal or usage tests. Conditions for these tests can be tightly controlled to provide the highest quality of scientific rigor. The disadvantage of in vitro tests is represented by their potential lack of relevance to the in vivo use of the material.

The animal tests place a material into an intact organism of an common animal (mice, rats, hamsters, ferrets, or guinea pigs) but many other types of animals have been used (eg sheep, monkeys, baboons, pigs, cats, and dogs).

Pulp studies and animal tests are distinct from in vitro tests. In the latter tests, an animal intact is used rather than cells/tissues from an animal. Animal tests are distinct from usage tests in that animal tests expose the animal to the material without regard to the material's final use.

The animal tests can be subdivided into several types: short-term or long-term systemic toxicity, exposure to intact or abraded membranes, and immune sensitization or bone response. There are also animal tests for mutagenicity, carcinogenicity and other specialized conditions.

The advantage of an animal test is its ability to allow an intact biological system to respond to a material. The material may interact with the many complex biological systems within the animal and a more complete biological response is therefore measured.

The animal tests are expensive and difficult to control, may take many months/even years to complete, depending on the species used. These tests are controversial because of ethical concerns about proper animal treatment. The relevance of an animal test is often questioned because of concerns about the ability of any animal species used to adequately represent the human species. The animal tests provide an important bridge between the in vitro environment and the clinical use of the material.

The usage tests are performed in animals/humans and require that the material should be placed in an environment clinically relevant to the use of the material in clinical practice.

If the test is realized in humans, is called “clinical trial” rather than a usage test. The choice of animals for a usage test will be more limited than for an animal test. Not all species can be used for all clinical situations because of the size or anatomy of a given species. Thus usage tests are more likely to be performed on larger animals with anatomy that more closely resembles that of humans. The relevance of a usage test to clinical practice is potentially high by definition. However, the ultimate relevance of a usage test depends directly on the quality with which the test mimics the clinical use of the material in terms of time area, clinical environment, and placement technique.

The human clinical trial is therefore the "gold standard" of usage tests and is the standard by which in vitro and animal tests are judged.

The usage tests have disadvantages: are very complex and difficult to perform in terms of experimental control and interpretation, are exceptionally expensive (if humans are to be used, must be obtained approval for clinical trial, from an Institutional Review Board), the time required for these tests may stretch from months to years if data on the long-term performance of a material are desired. Finally, human usage tests may involve many legal liabilities and issues that are not factors for animal and in vitro tests.

Generally, not a single test is used to evaluate the biocompatibility of a new material. Must be used together: in vitro, animal and usage tests.Three phases are generally recognized in the testing of a new biomaterial: primary, secondary, and usage.

Primary tests are performed initially in the testing of a new material; these tests are often in vitro in nature. Primary tests might also include some animal tests to measure systemic toxicity.

Secondary tests are almost always conducted in animals. These tests explore beyond toxicity/mutagenicity toward issues such as allergy, inflammation and other sub lethal and chronic biological responses. More sophisticated in vitro tests are being developed for inflammation, estrogenicity, surface effects, and osteoinduction. that are also secondary in nature.

The testing of a new material is a linear progression from primary to secondary to usage tests. Primary tests are conducted first and only the materials that pass these primary tests are tested in the secondary phase. Similarly, only materials that have favorable results in the secondary tests are subjected to usage tests.

The ANSI/ADA document 41 for biological testing of dental materials was updated in 1982 to include tests for mutagenicity. This specification uses the linear paradigm for materials screening and divides testing into initial, secondary and usage tests.

The initial tests include in vitro assays for cytotoxicity, red blood cell membrane lysis, mutagenesis, and carcinogenesis, animal tests for systemic toxicity by oral ingestion.

Secondary tests include animal tests for inflammatory or immune responses.

Usage tests include tests for pulpal and bone response. The required tests for a given material are not listed specifically. Rather, it is up to the manufacturer to select the tests and defend the selection to the ANSI/ADA and later to the FDA when applying for approval of the material.

The ISO 10993 document is the international standard for testing the biocompatibility of materials and is not restricted to dental materials. This document was first published in 1992, but modified versions are updated periodically. In 2002, ISO 10993 consisted of 16 parts, each addressing a different area of biological testing.

Two types of tests are covered in the standard: initial tests for cytotoxicity, sensitization, and systemic toxicity, and supplementary tests for chronic toxicity, carcinogenicity, and biodegradation. In addition, some specialized tests for devices are addressed, such as the dentin barrier test for restorative dental materials. The initial tests may be in vitro or animal tests, whereas the supplementary tests are performed on animals or humans. In this standard, usage tests are part of the supplementary tests. As with the

ANSI/ADA standard, the selection of tests is left to the manufacturer, who must then defend this selection upon application for approval.

The standardization of biocompatibility testing of materials has done much to advance understanding of biocompatibility and to protect the patients. Because the nature of biologic testing involves innumerable variables, standardization is critical to the unbiased comparison of results from different studies. In this sense, standards are very important. Standards have disadvantages: most of them cannot keep pace with the development of new scientific information, such as the rapid advance of-cellular and molecular biological techniques; standards represent a compromise among manufacturers, academicians, and the lay public; they tend to be developed slowly. Standards for biological testing are desirable and necessary for scientists, manufacturers, and patients.

In practice, no material can be shown to be 100% safe or risk-free. The dentist must recognize that the use of materials in the oral cavity requires a risk-benefit analysis. Only the use of biocompatible materials can assure the success of the dental treatment.

REFERENCES

Hussain, *Textbook of Dental Materials.* Ed. Jaypee Brothers Publishers, 2008.
O'Brien W.J., *Dental Materials and Their Selection.* Ed. Quintessence Pub. Co, 2008.
McCabe J.F., Walls A.. *Applied Dental Materials.* Ed. John Wiley and Sons, 2008.
Anusavice K.J., Phillips R.W., *Phillips' Science of Dental Materials.* Ed. Saunders, 2003.

ASPECTE PRIVIND BIOCOMPATIBILITATEA MATERIALELOR UTILIZATE ÎN STOMATOLOGIE

(Rezumat)

In medicină, biocompatibilitatea presupune o interacţiune între material şi corp. Aplicarea unei restaurări în cavitatea orală creează o interfaţă între material şi ţesuturile adiacente acestuia. Interfaţa există, este activă şi dinamică şi implică două modalităţi de interacţiuni prin care ţesutul poate influenţa materialul sau viceversa. În practica stomatologică există o serie de posibile reacţii biologice la materialele dentare (reacţii toxice, reacţii inflamatorii, reactii alergice, reactii mutagene). Utilizarea materialelor pentru refacerea structurilor dentare afectate sau pierdute creează medii speciale în care biocompatibilitatea materialului este primordială pentru supravieţuirea restaurării pe termen lung. Pentru măsurarea biocompatibilităţii materialelor dentare sunt folosite trei tipuri de teste, considerate de bază: testarea in vitro, testul pe animale, testul de utilizare, efectuat fie la animale sau la oameni. În practică, nici un material poate fi dovedit a fi 100% sigur sau lipsit de risc. Medicul dentist trebuie să recunoască faptul că utilizarea materialelor în cavitatea orală necesită o analiză risc-beneficiu. Numai utilizarea unor materiale biocompatibile poate asigura succesul tratamentului stomatologic.

BULETINUL INSTITUTULUI POLITEHNIC DIN IAȘI
Publicat de
Universitatea Tehnică „Gheorghe Asachi” din Iaşi
Tomul LVIII (LXII), Fasc. 1, 2012
Secția
ŞTIINȚA ŞI INGINERIA MATERIALELOR

CONSIDERATION REGARDING GRAIN GROWTH AND NUCLEATION ON SOLIDIFIED LAYERS DEPOSITED BY THERMAL SPRAYING

BY

TUDOR-BRIAN LANDKAMMER* and LAURA-TEODORA SOLONARIU[1]

“Gheorghe Asachi” Technical University of Iaşi
Faculty of Material Science and Engineering
[1]S.C. HIDROSERV “BISTRIȚA” S.A., Piatra Neamț

Received: January 25, 2012
Accepted for publication: February 29, 2012

Abstract: The solidification process includes nucleation and growing steps, each of them are being influenced by specific parameters. According to some specific condition, nucleation can be homogeneous or heterogeneous and it will assure the forming condition of a amorphous or crystalline microstructure.

Knowing the values of the technological parameters for spraying it is possible to determine the growing speed of a sprayed layer through mathematical calculation or by numerical simulation.

Keywords: thermal spraying; nucleation; crystal morphology; technological parameters.

1. Introduction

The solidification process of a thermally sprayed layer begins right after the contact between the splat and the metallic substrate. The resulting heat will be released through the cold substrate after it crosses the lamella formed on the substrate.

---

* Corresponding author: *e-mail*: tudor_brian@yahoo.com

The solidification process of splats may occur:

a) by deformation of the splat from the contact with the substrate surface;

b) simultaneously with the splat deformation;

c) before deformation of the splat begins.

The contact surface between the coating and the metallic substrate will be the initiation spot of the nucleation process. Solidification of the first sprayed liquid particles will have a heterogeneous character and the grains will grow like columns.

2. Specific Parameters of Nucleation and Grain Growth

The nucleation process is influenced by two main parameters: undercooling effect and thermal contact resistance.

The undercooling effect (ΔT) is represented by the difference between the theoretical temperature ($T_s = T_t$) and real temperature (T_r) of the solidification process. The undercooling effect of heterogeneous solidification is lower than the one for homogeneous solidification. Dyshlovenko (Dyshlovenko *et al.*, 2006) showed that, for hydroxyapatite spraying, if the particles solidify before they reach the substrate surface the undercooling effect is:

$$\Delta T = (0.12 \ldots 0.14)\, T_t \tag{1}$$

Wilden (Wilden *et al.*, 2001) noticed that dendrite structure formed through solidification is finer for lower values of undercooling effect.

The thermal contact resistance formed at the interface between splats and substrate acts as a thermal barrier of latent heat evacuation from the solidification process. This resistance is characterized by a variation of its value in different points of the splat/substrate interface but also in different points of splat/sprayed layer interface (Fig. 1).

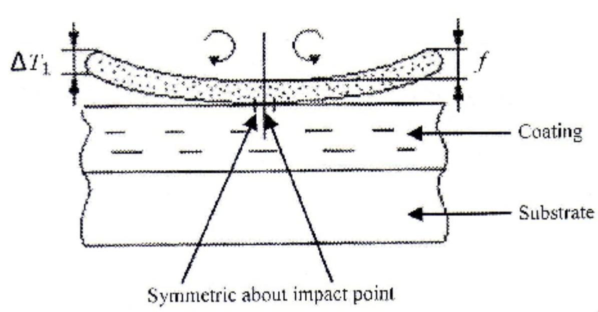

Fig. 1 – Curling of the splats surface

Curling with a certain amount (f) of upper and lower part of the splat surface is determined by a difference of temperature between them.

2.1. The Morphology of Formed Crystals

According to the cooling speed of the splat material the solidification front can be planar, cellular or dendritically.

In the case of heterogeneous nucleation a high cooling speed and a planar front of solidification is needed. Based on the value of undercooling effect the solidification front speed can be measured in [cm/s] or [m/s].

Towards the end of solidification an increase of the liquid phase temperature is noticed as a function of recalescence point (Fig. 2), which will favor the formation of a columnar structure (Fig. 3).

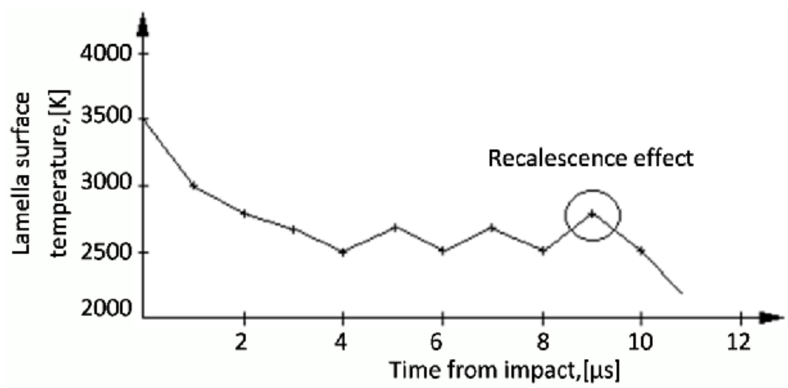

Fig. 2 – The evolution of front temperature solidification of a niobium splat, arc plasma sprayed using powder having a particle size of 22.5 µm.

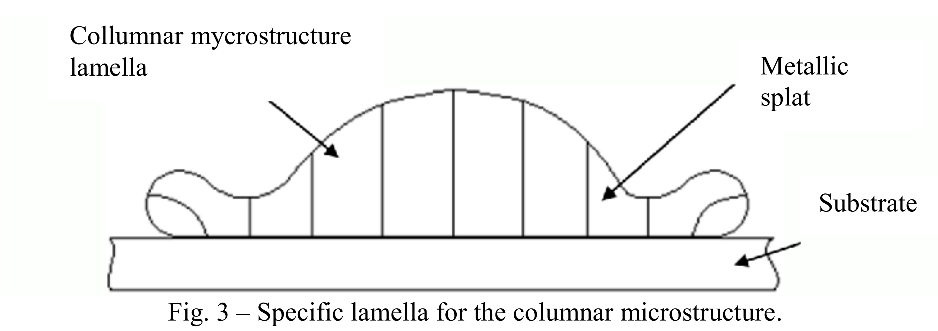

Fig. 3 – Specific lamella for the columnar microstructure.

Recent studies showed that the density of formed columnar grains, on the sprayed layer, depends on its surface temperature. Robert et al. /6/ determined a density of 20…80 grains/µm^2 in the case of alumina spraying with the APS method. The subsequent AFM analyzes confirm these calculated values.

In numerous cases the microstructure of the sprayed layer presented fine and equiaxial grains (Fig. 4).

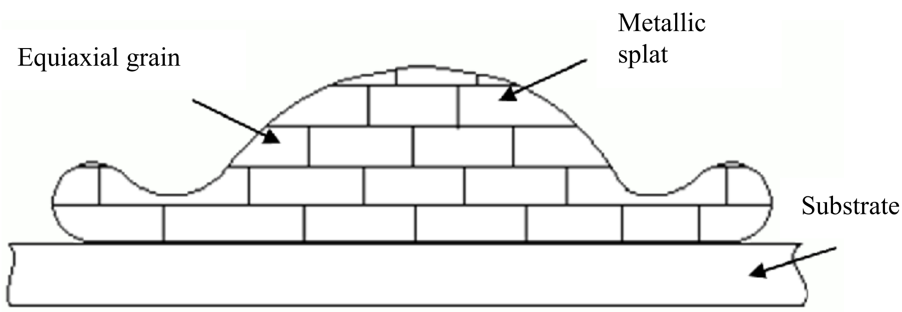

Fig. 4 – Fine and equiaxial grain with a "brick wall" microstructure.

Formation of an equiaxial microstructure is favored by low speed heat dissipation at the substrate interface. In this case, the nucleation becomes heterogeneous and the subcooling effect will be more intense. The fine and equiaxial grains were observed in the microstructure obtained by APS spraying of molybdenum and Al_2O_3+Y_2O_3 particles. Safai and Herman (1981) identified a microstructure with equiaxial character in the center zone of an alumina lamella formed by APS spraying.

It is possible that a brick wall microstructure is obtained by recrystallization of the spayed layer. This aspect was observed by Sampath and Herman (1989), with the nickel layers sprayed by VPS, in which situation the high temperature of the substrate allowed recrystallization to occur. Recrystallization of the sprayed layer was also recorded in the case of VPS spraying of copper particles.

2.2. Formation of a Amorphous and an Orientated Microstructure

If in the cooling process no nucleation center is formed then by the end of the solidification, an amorphous microstructure will be obtained. The obtainment of this type of microstructure can be influenced by:

a) assuring a high speed cooling of the sprayed layer;
b) adding in the spraying flow of Y_2O_3 or SiO_2 particles.

The existence of an amorphous phase was observed by Wilms and Herman (1976) at spraying yttrium and alumina layers near the interface between the propelled particle and substrate were the cooling speed is at a maximum.

In the case of high speed solidification, a preferred direction of crystal growth is possible. Identification of a textured solidification will be permitted by the development of a preferential orientated columnar grain microstructure on a perpendicular direction to the substrate. It has been observed that on Ni and

Ni-Al spraying an orientated texture on the <200> direction is formed. The surface preparation method will influence the possibility of obtaining a textured surface. It was noticed that high roughness obtained by sand blasting adversely influences the formation of a textured solidification pattern.

The grain size formed in the thermally sprayed layer vary between $10^{-6}...10^{-9}$ mm. Thermally spraying a hardened steel or an liquid nitrogen cooled steel, so that the temperature reaches 100 K, will allow the obtainment of nanometric grains of Feα (BCC) of 3…10 nm.

3. Coating Growth

3.1. Mechanism of Coating Growth

A section of a thermally sprayed coating displays many lamellae piled up one upon another, as shown in Fig. 5.

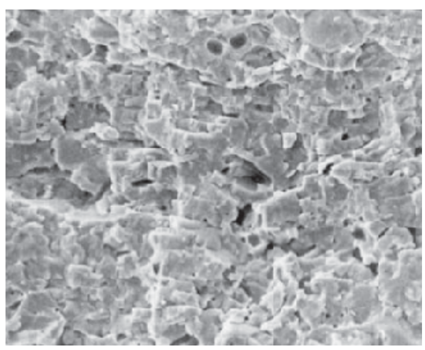

Fig. 5 – Scanning electron microscopy of a fractured section of an Al_2O_3 coating obtained by APS (Pawlowski).

Al_2O_3 lamellae have a thickness of about 4 µm which let us find the flattening parameter, which is equal to 2.4. The area covered by a lamella is about 4900 µm^2. Knowing the powder feed rate (65g/min) and supposing that 50% of the particle striking the substrate stick to it, the number of particle being deposited on the substrate during one second is 6.85×10^6. The lamellae formed therefore will be placed near to each other and will cover an area of 335.65 cm^{-2}.

Because a typical spray spot has a diameter of 2.5 cm and a spraying area of 4.9 cm^2 then in one second as many as 68.5 lamellae will be formed on top of each other and the coating will increase in thickness with 274 µm/s.

The spraying torch can move with different linear velocity with regard to the substrate which will influence the number of lamellae formed in one layer.

Knowing that for coating with alumina a 43kW electric power was needed and that the spraying distance was 90 mm it was possible to determine the linear velocity for the spraying torch. From the experimental point of view the following results were obtained, table 1.

Table 1
Values of Characteristics Coatings for Different Linear Velocities (Pawlowski)

Linear velocity mm/s	No. of lamellae in one layer	Thickness of the coating sprayed in one pass,[μm]
450	3.8	15
900	1.9	7.6
1,800	0.9	3.6

It is noticed that using high linear velocities leads to obtaining low thickness coating. Increasing the linear velocity will lead to shortening the time between layer spraying and also will decrease the time of exposure of the sprayed layer to the ambient. In this manner the temperature variation between the first and last sprayed layer will be limited therefore obtaining a favorable effect on the internal residual tensions.

The value of linear velocity will be obtained according to the physical properties of the sprayed material and of the exterior geometry of the sprayed surface.

Because zirconium has a high thermal expansion coefficient one can use wider value intervals without generating major internal tension. In the case of coating ceramics on metallic substrates it is recommended the usage of high linear velocities.

On coating cylindrical surfaces it is recommended that the linear velocity is split into two components: linear velocity of the spraying head and the rotation speed of the metallic piece. The recommended values for the specific parameters of this practical application are presented in Table 2.

Table 2
Linear Velocities and Rotation Values as a Function of the APS Sprayed Cylindrical Diameter of Samples (Pawlowski)

Cylinder diameter mm	Rotation speed rot/min	Linear velocity mm/s
50	689	46
100	343	23
150	229	15
200	172	11
250	137	9
300	115	8

Note: The linear advance motion of the gun is 4 mm/rot.

The powder sprayed on the substrate has spatial distribution and a Gaussian aspect. The distribution becomes diffused once the distance between the gun and the surface is increased. To avoid the occurrence of periodical variation in thickness of the sprayed layer it is of most importance to correctly choose the value of the three parameters so that it can reduce the number of passes of the gun in order to obtain the require thickness.

The process of coating growth can be numerically simulated. The first 2D studies were made by Knotek and Elsing (1987) using the Monte Carlo method. Subsequently Cirolini (1991) and Doltsinis (1998) took into account different situation obtained from the impact between the liquid sprayed particle and the metallic substrate. With some modifications the obtained simulation software was used to analyze hydroxyapatite coating growth sprayed by APS.

Wei (2004) designed the 3D model for ZrO_2 layer growth obtained by thermal spraying and Xue (2004) established the 3D model that can reproduce nickel layer growth sprayed in plasma (APS).

4. Conclusions

1. The value of the undercooling effect influences the nucleation and growing processes of the sprayed layer. The dimension of the dendrites formed by solidification is finer when the undecooling effect is lower.

2. Thermal contact resistance acts as a barrier for evacuating the latent heat of the solidification process. It presents numerical variations at the interface between the liquid sprayed particle/substrate or liquid sprayed particle/previously sprayed layer.

3. The undecooling effect will influence the shape and speed of the solidification front. Recalescence phenomenon will favor a columnar microstructure forming.

4. Slow dissipation of solidification latent heat ensures proper conditions for heterogeneous nucleation and the forming of a brick wall microstructure with fine and equiaxial grains.

5. The lack of nucleation cores will lead to the formation of a amorphous microstructure, while a high speed solidification results in obtaining columnar grains with similar crystallographic orientation (solidification texture).

6. Based on the values of adopted technological parameters of the thermal spraying process it is possible to determine the growing speed of a sprayed layer.

7. Linear velocity of the spraying torch will influence the thickness of the sprayed layer. Higher values of this parameter will result in obtaining thinner layers and with lower internal tensions.

8. For spraying cylindrical surfaces, choosing the correct rotation speed and linear velocity will enable obtaining required thickness of the sprayed layer.

There are 2D and 3D models for simulating growing process of a layer as a function of work technological parameters.

REFERENCES

Cirolini S., Harding J.H., Jacucci G., *Computer Simulation of Plasma Sprayed Coatings*. I. *Coating Deposition Model*. Surf. Coat. Technol., **48**, 137-145 (1991).

Doltsinis I.S., Harding J., Marchese M., *Modelling the Production and Performance Analysis of Plasma-Sprayed Ceramic Thermal Barrier Coatimg*. Arch. Comput. Meth. Engng., **5**, 59-166 (1998).

Dyshlovenko S., Pawlowski L., Pateyron B., Smurov I., Harding J.H., *Modeling of Plasma Particles Interactions and Coating Growth for Plasma Spraying of Hydroxyapatite*. Surf. Coat. Technol., **200**, 3757-3769 (2006).

Knotek O., Elsing R., *Monte Carlo Simulation of the Lamellar Structure of Thermally Sprayed Coating*. Surf. Coat. Technol., **32**, 261-271 (1987).

Pawlowski L., *The Science and Engineering of Thermal Spray Coatings* (Second Edition). John Wiley & Sons Ltd, The Atrium, 2008

Robert C., Denoirjean A., Vardelle A., Wang G-X., Sampath S., *Nucleation and Phase Selection in Plasma Sprayed Alumina: Modeling and Experiment*. Thermal Spray: Meeting the Challenges of the 21st Century, ASM Internat., C. Coddet (Ed.), 407-412, Materials park, OH, USA, 1998.

Safai S., Herman H., *Plasma Sprayed Materials*. Treatise on Mater. Sci. a. Technol., **20**, Academic Press, 183-213, New York, NY, USA, 1981.

Sampath S., Herman H., *Microstructural Development of Plasma Sprayed Coatings*. Proc. of the 12th Internat. Thermal Spray Conf., The Weleding Inst., Cambridge, UK, 1989, 53.

Wei G., Xiong H., Zheng L., Zhang H., *An Advanced Ceramic Coating Buildup Model for Thermal Spray Processes*. Proc. of the Internat. Thermal Spray Conf. ’04, DVS-Verlang, Düsseldorf, Germany, 2004.

Wilden J., Frank H., Müler T., *Microstructure Simulation of Thermally Sprayed Particles*. Thermal Spray 2001: New Surfaces for a New Millennium, ASM Internat., C. C. Berndt (Ed.), 875-882, Materials Park, OH, USA, 2001.

Wilms V., Herman H., *Plasma spraying of* $Al_2O_3 – Y_2O_3$. Thin Solid Films, **39**, 251-262 (1976).

Xue M., Mostaghini J., Chandra S., *Prediction of Coating Microstructure*. Proc. of the Internat. Thermal Spray Conf. ’04, DVS-Verlag, Düsseldorf, Germany, 2004.

CONSIDERAȚII PRIVIND GERMINAREA ŞI CREŞTEREA GRĂUNȚILOR LA SOLIDIFICAREA STRATURILOR DEPUSE PRIN PULVERIZARE TERMICĂ

(Rezumat)

Procesul de solidifcare include etapele de germinare şi creştere, fiecare dintre ele fiind influențate de parametrii specifici. În funcție de condițiile specifice, germinarea

va putea fi omogenă sau eterogenă şi ea va asigura condiții pentru formarea unei microstructuri cristalină sau amorfă. Cunoscând valorile parametrilor tehnologici de pulverizare este posibilă determinarea vitezei de creştere a unui strat depus atât prin calcul matematic, cât şi prin simulare numerică.

BULETINUL INSTITUTULUI POLITEHNIC DIN IAȘI
Publicat de
Universitatea Tehnică „Gheorghe Asachi” din Iaşi
Tomul LVIII (LXII), Fasc. 1, 2012
Secția
ŞTIINȚA ŞI INGINERIA MATERIALELOR

MAGNESIUM ALLOYS AS BIODEGRADABLE IMPLANTS

BY

OANA BĂLȚĂTESCU*, IOAN CARCEA and RALUCA FLOREA

“Gheorghe Asachi” Technical University of Iaşi
Faculty of Material Science and Engineering

Received: March 19, 2012
Accepted for publication: March 29, 2012

Abstract: Applications of magnesium alloys as biodegradable orthopaedic implants are critically dependent on the mechanical integrity of the implant during service. Magnesium alloys offer a very high specific strength among conventional engineering alloys. In addition, magnesium alloys possess good damping capacity, excellent castability, and superior machinability.

Keywords: composite; bioabsorbable; biodegradable; magnesium.

1. Introduction

Since 1945, when the engineers used for the first time magnesium alloys as anode for cell production, they have been continuously to improved and optimize the electrochemical characteristics. Magnesium alloys have attracted much attention as potential biodegradable bone implant materials due to their biodegradability in the bioenvironment (Witte *et al*., 2005, 2006; Xu *et al*., 2007), and their excellent mechanical properties such as high strength and possessing an elastic modulus close to that of bone (Staiger *et al*., 2006). However, the rapid corrosion of magnesium alloys in chloride containing solutions including human body fluid or blood plasma has limited their clinical

* Corresponding author: *e-mail*: oana84rou@yahoo.com

applications (Staiger *et al.*, 2006; Song *et al.*, 2010). Therefore, it is very important to improve the corrosion resistance of magnesium alloys in order for them to be applied clinically.

Magnesium is an element essential to human body. Intake of a certain amount of magnesium (300–400 mg/day) is normally required for the human body's metabolic activities. The direct corrosion product of magnesium, Mg^{2+}, would be easily absorbed or consumed by the human body. No side effect of Mg^{2+} overdose has been found in human body (Song *et al.*, 2010). Hydrogen evolution and alkalization resulting from Mg corrosion are the most critical obstacles in using magnesium as an implant material.

Materials science has contributed to the practice of surgery since the earliest procedures were performed and the first implants placed. Although there have been reports of biomaterial use dating back over 32,000 years, most of the biomaterial applications have occurred over the past 2,000 years. Examples of these early materials include wooden teeth, glass eyes, and metallic dental implants. The modern age of biomaterial science started in the late 1,800 s with two key innovations: the implementation of aseptic techniques reducing the potential of infection-related complications and the radiograph techniques pioneered by Roentgen allowing for visualization of skeletal structures (Bhat, 2005).

2. Classification

Composite materials, generally, could be calssified in metal, ceramic, organic and polymeric matrix composites. Magnesium based composites are from the group of metals matrix composites. These materials can be classified by the:

a) *field of use*.

It is well known the fact that magnesium composites are used in medical applications. The development of biodegradable orthopedic implants has been one of the important areas in biomedical engineering. Biodegradable and biocompatible implants can gradually be dissolved and absorbed in the human organism after implantation. From these point of view magnesium (Mg) and its alloys are among the most interested options.

Another application of Mg based composites is for manufacturing galvanic cells, because of their electrode potential and specific ability. But, these alloys have the disadvantage of inherent inhomogeneity of the materials obtained by conventional metallurgical operations and a lower corrosion resistance. These materials are used in the manufacture of sea water activation galvanic elements, of weld-brazing and welding electrodes for the "Electron" type alloys, of „honeycomb" type composites from ultra-rapidly solidified magnesium alloy ribbons, as well as in the development of materials suitable to store hydrogen used as an alternative energy source.

Due to their lightweight magnesium alloys have been increasingly used in the automotive industry.

b) *number of alloying elements*.

From this point of view there are four gropus of magnesium based metal matrix composites: binary alloys (*e.g*. Mg-Nd, Mg-Zn, Mg-Ca, Mg-Zr, Mg-RE, Mg-Al, Mg-Li, Mg-Y, etc.); ternary alloys (*e.g*. Mg-Mn-Zn, Mg-Zn-Sr, etc.); quaternary alloys (*e.g*. Mg-Nd-Zn-Zr, Mg–Y–Nd–HRE, Mg-Th-Zn-Zr, Mg-Nd-Ag-Pb, Mg-Al-Zn-Pb, etc.) and complexes alloys.

1) Mg-Al alloy system (Witte *et al*., 2005) had reported that the implantation of AZ31 and AZ91 alloy sample rods, compared to the polymer, increased the newly formed bone, and the corrosion layer of both alloys displayed an accumulation of biological calcium phosphates. Zijian *et al*. (2008), had reported that the degradation of AE21 stent (4 mg) in coronary artery was considered to be linear and drew the conclusion that the vascular implants consisting of magnesium alloys seemed to be a realistic alternative to permanent implants.

2) Mg-RE alloy system. The in vivo corrosion of LAE442 and WE43 were also investigated by Witte *et al.* (2005), with the same procedure as that of AZ31 and AZ91. A much slow corrosion rate was recorded for LAE442, while AZ31, AZ91 and WE43 were found to degrade at similar rates. A Biotronik's Mg absorbable metal stent (AMS) (with 10 wt% of rare earth) had been successfully used in one preterm baby with an artificial pulmonary artery stenosis and the 4-month degradation process was clinically well tolerated, despite the small size of the baby. However, another case of the implantation of AMS stent into a newborn with severely impaired heart function due to a long segment recoarctation after a complex surgical repair was not well tolerated (Mani *et al*., 2007).

c) *processing techniques*.

From this point of view, Mg based metal matrix composites could be devided into:

a) Magnesium based metal matrix composites produced by technology derived from powder metallurgy.

b) Magnesium based metal matrix composites produced by technology derived from the processes of casting alloys.

c) Magnesium based metal matrix composites produced by ultra-rapid solidifications.

d) Magnesium based metal matrix composites produced by spray deposition technologies.

3. Field of Use

Magnesium alloys have been increasingly used in the automotive industry in recent years due to their lightweight. The density of magnesium is approximately two thirds of that of aluminum, one quarter of zinc, and one fifth of steel. As a result, magnesium alloys offer a very high specific strength among conventional engineering alloys. In addition, magnesium alloys possess good damping capacity, excellent castability, and superior machinability. Accordingly, magnesium casting production has experienced an annual growth of between 10% and 20% over the past decades and is expected to continue at this rate (Hai *et al*., 2004).

Magnesium has shown potential application as a bio-absorbable biomaterial, such as for bone screws and plates. Element alloying has been studied for developing biodegradable magnesium alloys with good mechanical and corrosion properties. Mn and Zn were selected as the alloying elements to develop Mg-Mn-Zn alloys due to the good biocompatibility of Mn and Zn (Yin *et al*., 2008; Zhang & Zeng, 2008). The addition of Mn and Zn improves both the mechanical properties and the corrosion resistance of magnesium alloys. Most of conventional orthopaedic implants used for repairing joint and bone fractures consist of metallic biomaterials with polycrystalline microstructure that exhibit good corrosion resistance, high hardness and excellent fatigue and wear resistance.

The need for a bone adhesive that can be used in fracture repair and trauma surgery remains unmet despite over half a century of work in this area. Initial attempts largely focused on taking adhesives developed for engineering or other applications and applying them to bone with a, perhaps unsurprising, lack of success. More recently, we have seen more rational attempts to design adhesives specifically aimed at bone repair as well as approaches based on mimicking nature's own adhesive systems. Nevertheless, the challenges faced in developing a bone adhesive remain substantial, with many (sometimes conflicting) require- ments having to be taken into account. Another problem is the general lack of consensus and consistency in how to test such adhesive systems–both *in vitro*/*exvivo* and *in vivo*. However, progress is being made on a number of fronts and hopefully, in the not too distant future, orthopaedic surgeons will be able to add glue to their toolkit for repairing broken bones.

Reabsorbable bioceramics degrade over time and are replaced by endogenous tissues resulting in normal, functional bone when used in orthopedic applications. Their osteoconductive ability, or ability to allow for osteoblast integration leading to osteoid formation, is a key property. Materials including calcium phosphates, hydroxyapatite, and calcium sulfate dihydrate (plaster of paris) are classified as reabsorbable bioceramics. The degradation and osteoid formation rates are variable and depend on the type of material. Typically, the mechanical properties of these materials are greatly reduced during the reabsorption process, resulting in a significantly different load-bearing capacity over the course of integration. The use of reabsorbable scaffolds seeded with cells has been used for tissue engineering applications and has the potential to behave as a synthetic extracellular matrix. The ability of a material to chemically bond and interact with normal tissue at its interface is the key characteristic of *bioreactive* bioceramics. Bioglass and Ceravital are classified as bioreactive materials and are typically used as bone cement fillers, interfacial coatings for implants, and restorative composites. The presence of these materials as the bulk implant or in the form of coatings on other materials causes the surrounding tissues to bind with them, providing better integration and less residual stress at the interface. The ability to incorporate themselves makes surface reactive bioceramics difficult to extract once they have healed into place (Velikokhatnyi and Kumta, 2010).

4. Conclusions

Material science has been described as part of a health care puzzle that will be driven by clinical need, with the ultimate goal of being able to replace function in part of a failed organism through the use of biomaterial science. Advancements will result from interdisciplinary efforts that require the combination of fields and the collaboration of experts with the ultimate goal of manipulating and maintaining the very complex physiological system known as the human body. Clinicians play a key role in that process and should continue to pioneer material science applications in patient treatment.

As an essential element in the human body, Mg shows good biocompatibility as well as no toxicity, and its degradation in human body environment could avoid the second removal surgical operation. In addition, Mg is relatively abundant in natural resource with low price, and is well regarded to play an important role in human metabolism as well as the properties of human bones.

The major disadvantage of Mg alloys as biodegradable implant materials is that pure Mg is prone to corrode too quickly at physiological environments and to degrade its mechanical integrity before the tissue has sufficiently healed.

In medical field biodegradable magnesium alloy achieves enhanced bone response and excellent interfacial strength and thus fulfils two critical requirements for bone implant applications. Magnesium based alloy seems to hold great potential for bone implant applications.

REFERENCES

Bhat SV. *Biomaterials* (Second Edition). Alpha Sci. Internat., Harrow, U.K., 2005.

Hai Z.Y., Xing Y.L., *Review of Recent Studies in Magnesium Matrix Composites*. J. of Mater. Sci., *39*, 6153-6171 (2004).

Mani G., Feldman M.D., Patel D., Agrawal M., *Coronary Stents: a Materials Perspective*, Biomaterials, *28*, 1689-1710 (2007).

Song Y., Zhang S., Li J., Zhao C., Zhang X., *Electrodeposition of Ca–P Coatings on Biodegradable Mg Alloy: in Vitro Biomineralization Behaviour*. Acta

Biomaterialia, *6*, 1736-1742 (2010).
Staiger M.P., Pietak A.M., Huadmai J., Dias G., *Magnesium and its Alloys as Orthopedic Biomaterials: a Review*, Biomater., **27**, *9*, 1728-1734 (2006).
Witte F., Fischer J., Nellesen J., Crostack H.A., Kaese V., Pisch A. *et al*., *In Vitro and in Vivo Corrosion Measurements of Magnesium Alloys*. Biomaterials, **27**, *7*, 1013-1018 (2006).
Witte F., Kaese V., Haferkamp H., Switzer E. *et al*., *In Vivo Corrosion of Four Magnesium Alloys and the Associated Bone Response*. Biomaterials, **26**, *17*, 3557-3563 (2005).
Xu L., Yu G., Zhang E., Pan F., Yang K., *In Vivo Corrosion Behavior of Mg-Mn-Zn Alloy for Bone Implants Application*. J. Biomed. Mater. Res., **83A**, *3*, 703-711 (2007).
Yin D., Zhang E., Zeng S., *Effect of Zn on Mechanical Property and Corrosion Property of Extruded Mg-Zn-Mn Alloy*. T. Nonferrous. Metal. Soc., **18**, *4*, 763-778 (2008).
Zhang E., Zeng S., *Effect of Zn on Mechanical Property and Corrosion Property of Extruded Mg-Zn-Mn Alloy*. T. Nonferrous. Metal. Soc., **18**, *4*, 763-778 (2008).
Zijian L., Xunan G., Siquan L., Yufeng Z., *The Development of Binary MgeCa Alloys for Use as Biodegradable Materials Within Bone*. Biomaterials, *29*, 1329-1344 (2008).

ALIAJE DE MAGNEZIU PENTRU IMPLANTURI BIODEGRADABILE

(Rezumat)

Utilizarea aliajelor de magneziu pentru implanturi ortopedice biodegradabile este extrem de dependentă de integritatea mecanică a implantului în timpul serviciului. Aliaje de magneziu oferă o rezistență foarte mare față de alte aliaje inginerești convenționale. În plus, aliaje de magneziu posedă o turnabilitate excelentă şi prelucrabilitate mecanică superioară.

BULETINUL INSTITUTULUI POLITEHNIC DIN IAŞI
Publicat de
Universitatea Tehnică „Gheorghe Asachi” din Iaşi
Tomul LVIII (LXII), Fasc. 1, 2012
Secţia
ŞTIINŢA ŞI INGINERIA MATERIALELOR

DIFFERENTIAL SCANNING CALORIMETRY OF DIFFERENT METALLIC AND NON-METALLIC MATERIALS EXPERIMENTAL RESULTS

BY

IULIAN CIMPOEŞU*, **SERGIU STANCIU, ALEXANDRU ENACHE, MIHAELA RĂŢOI and RAMONA CIMPOEŞU**

"Gheorghe Asachi" Technical University of Iaşi
Faculty of Material Science and Engineering

Received: February 28, 2012
Accepted for publication: March 19, 2012

Abstract: Differential scanning calorimetry technique was used to analyze different metallic and non-metallic materials under thermal variation. Twelve materials like shape memory alloys, dental materials, special and super alloys, ceramics or magnesium hybrid were analyzed through differential scanning calorimetry under heating and cooling cycles and the results presented and comment. Different temperatures scales and dsc heating conditions were used to characterize few materials and to realize a starting database of dsc results.

Keywords: differential scanning calorimetry; shape memory alloys; dental materials.

1. Introduction

Differential scanning calorimetry or DSC is a thermoanalytical technique in which the difference in the amount of heat required to increase the temperature of a sample and reference is measured as a function of temperature.

---

* Corresponding author: *e-mail*: cimpoesuiulian@yahoo.com

Both the sample and reference are maintained at nearly the same temperature throughout the experiment. Generally, the temperature program for a DSC analysis is designed such that the sample holder temperature increases linearly as a function of time. The reference sample should have a well-defined heat capacity over the range of temperatures to be scanned.

The technique was developed by E.S. Watson and M.J. O'Neill in 1962 and introduced commercially at the 1963 Pittsburgh Conference on Analytical Chemistry and Applied Spectroscopy. The first adiabatic differential scanning calorimeter that could be used in biochemistry was developed by P.L. Privalov and D.R. Monaselidze in 1964. The term DSC was coined to describe this instrument which measures energy directly and allows precise measurements of heat capacity (Wunderlich, 1990).

The basic principle underlying this technique is that when the sample undergoes a physical transformation such as phase transitions, more or less heat will need to flow to it than the reference to maintain both at the same temperature. Whether less or more heat must flow to the sample depends on whether the process is exothermic or endothermic. For example, as a solid sample melts to a liquid it will require more heat flowing to the sample to increase its temperature at the same rate as the reference. This is due to the absorption of heat by the sample as it undergoes the endothermic phase transition from solid to liquid. Likewise, as the sample undergoes exothermic processes (such as crystallization) less heat is required to raise the sample temperature.

By observing the difference in heat flow between the sample and reference, differential scanning calorimeters are able to measure the amount of heat absorbed or released during such transitions. DSC may also be used to observe more subtle phase changes, such as glass transitions. It is widely used in industrial settings as a quality control instrument due to its applicability in evaluating sample purity and for studying polymer curing (Dean,1995; Pungor, 1995; Skoog *et al*., 1998).

Differential scanning calorimetry can be used to measure a number of characteristic properties of a sample. Using this technique it is possible to observe fusion and crystallization events as well as glass transition temperatures *Tg*. DSC can also be used to study oxidation, as well as other chemical reactions (Dean,1995; Pungor, 1995; Skoog *et al*., 1998; O'Neill, 1964).

Glass transitions may occur as the temperature of an amorphous solid is increased. These transitions appear as a step in the baseline of the recorded DSC signal. This is due to the sample undergoing a change in heat capacity; no formal phase change occurs (Dean,1995; Skoog *et al*., 1998).

As the temperature increases, an amorphous solid will become less viscous. At some point the molecules may obtain enough freedom of motion to spontaneously arrange themselves into a crystalline form. This is known as the crystallization temperature (*Tc*). This transition from amorphous solid to crystalline solid is an exothermic process, and results in a peak in the DSC signal. As the temperature increases the sample eventually reaches its melting temperature (*Tm*).

The melting process results in an endothermic peak in the DSC curve. The ability to determine transition temperatures and enthalpies makes DSC a valuable tool in producing phase diagrams for various chemical systems (Dean,1995).

2. Experimental Details

The DSC 200 ***F3*** *Maia*®, Differential Scanning Calorimeter, combines the advantages of modern technology, high sensitivity and a robust, easy-to-operate work horse. Using liquid nitrogen, the temperature range extends from -170°C to 600°C. The main features of the DSC 200 ***F3*** *Maia*® are the newly developed monolithic DSC sensor and a new silver furnace with long-life heating element. The heat flux sensor of the DSC 200 ***F3*** *Maia*®, Differential Scanning Calorimeter, combines high stability, improved resolution and fast response time. Laser-guided welding processes for the sensor disk and thermocouple wires yield high sensitivity and robustness.

For routine applications we offer the upgrade with an automatic sample changer (ASC) for up to 20 samples and reference materials, also in different crucible types. The concept of the new DSC 200 ***F3****Maia*, Differential Scanning Calorimeter, is tailored to routine applications in quality control, failure analysis and process optimization, especially in polymer processing. The DSC measuring cell consists of a cylindrical high-conductivity silver block with an embedded heating coil for broad thermal symmetry (3D symmetry) in the sample chamber, the cooling ports for liquid nitrogen or compressed air cooling and a cooling ring for connection of the intracooler (also with simultaneous liquid nitrogen cooling). The gas-tight construction and integrated mass flow controllers for the purge and protective gases allow coupling to an FTIR or MS for gas analysis.

With its disk-shaped silver carrier plate and supersensitive thermosensors of nickel-chromium constantan, the Tau-sensor offers a high level of calorimetric sensitivity along with extremely short signal time constants of only 0.6 s, which guarantees good separation of overlapping thermal effects. The μ-sensor stands out for its high level of calorimetric sensitivity, never before achieved with a Differential Scanning Calorimeter, DSC. For example, it is extremely well suited for pharmaceutical applications with small sample weights.

3. Experimental Results

When a sample of SMA (shape memory alloy) was deformed from its "original" state, it regains its original geometry by itself during heating (one-way effect) or at temperatures higher that room temperature, simply during unloading (pseudo-elasticity). These extraordinary properties of metallic material are due to temperature-dependent transformation from a low state of symmetry martensitic phase to a highly symmetric crystallographic structure. These crystals are known as martensitic and austenitic phases.

Range of applications for shape memory alloys has increased in recent years, with a major area of application: as an example in medicine the development of dental wires (braces) that exert constant pressure on the teeth at the average temperature in the mouth. However these materials are not always suited for applications such as actuators in robotics and artificial muscles because of energy inefficiency and slow reaction time and, in this case, a greater hysteresis, that's why are more suited to the dissipation of mechanical energy into heat or damping.

A differential scanning calorimetry (DSC) test was performed in the temperature range –50 to 50°C with a heating rate of 10 K/min in a nitrogen atmosphere 40 mL/min for a 5.34 mg sample mass in drilling aluminum crucible. Calorimetric analysis result is shown in Fig. 1 to highlight the left of the direction of exothermic transformation.

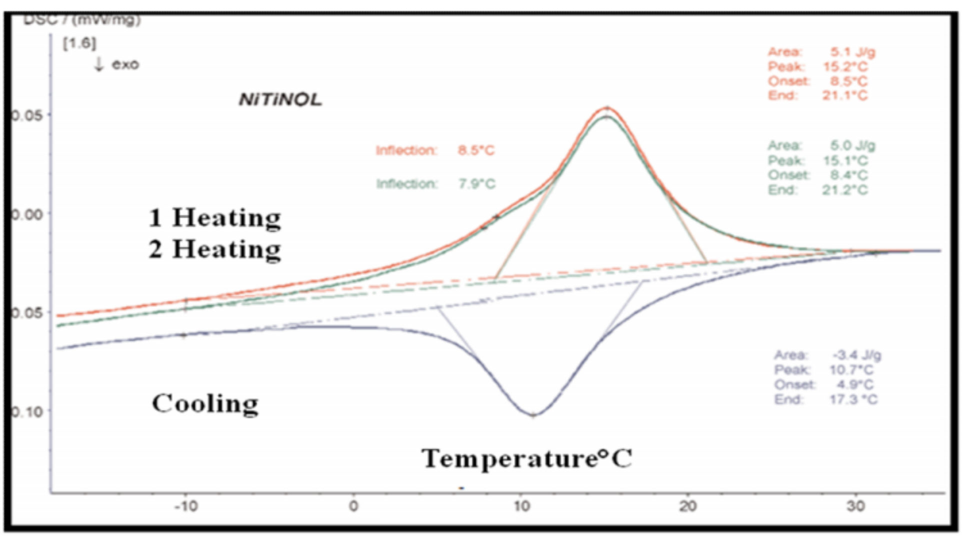

Fig. 1 – The behavior of a nitinol based shape memory alloy on heating calorimetric analysis (DSC).

Extraordinary properties of shape memory alloys are based on structural changes. Each phase transition is associated with a heat exchange and therefore can be studied by DSC calorimetric analysis. Shape memory alloys analysis with several cycles of heating and cooling establishes not only the phase transition temperature, but also proves the reversibility of these phase transitions. Comparing the results obtained after the first and second heating process confirms the peak identical form in both cases and reversible transition temperature values, but also for the transformation enthalpy.

The interesting field of smart materials is rapidly expanding and one of the most interesting areas is that of shape memory alloys. A shape memory alloy (SMA) may undergo substantial plastic deformation, and then be triggered to return to its original shape by applying a heat flux. Since the beginning of these applications, such as the greenhouse window opening item in which a SMA slide was the actuator temperature-dependent ventilation provided by the mobile antennas made of superelastic SMA, the list of requests for applications shape memory alloys has increased enormously in the 1990s. Medical applications of shape memory alloys using their super-elasticity property and shape recovery properties are particularly interesting and are rapidly developing.

It was developed a differential scanning calorimetric test (DSC) in the range temperature RT (room temperature) –1,000 °C with a heating rate of 10 K/min in an argon atmosphere of 50 mL/min for a 194.4 mg sample in a platinum crucible drilling aluminum insert. Calorimetric analysis result is shown in Fig. 2 and highlights in the left of exothermic transformation direction.

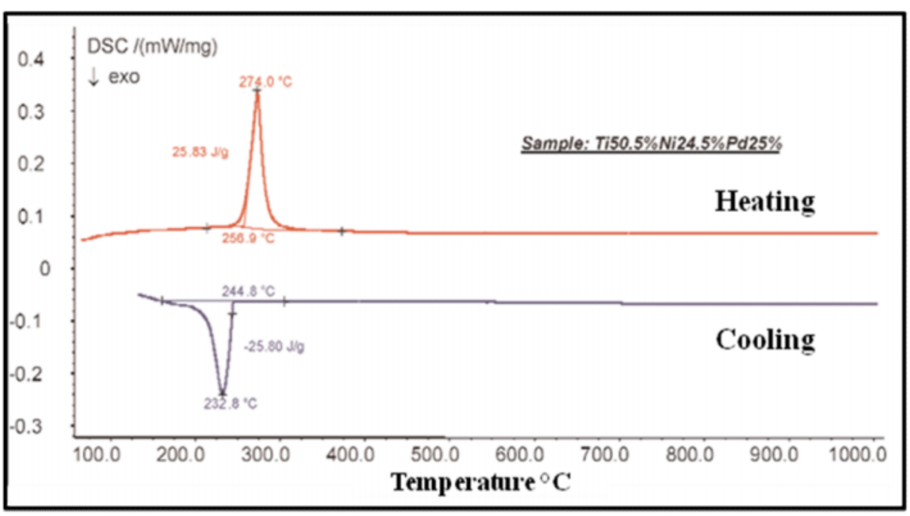

Fig. 2 – The behavior of a heated TiNiPd smart alloy with the calorimetric analysis (DSC).

Using a DSC system of calorimetric analysis running in a high purity atmosphere and to high temperatures, solid state transitions that occur in shape memory alloys at high temperatures can be studied without the disturbing influence of the oxidation phenomenon. In the considered alloy, changing the state of solid-solid transition is visible at 257°C temperature during heating and the 245°C temperature on cooling curve. Enthalpy change of solid phase transition was about 25.8 J/g.

Steel is a metal alloy whose major component is iron alloyed with carbon primarily. Chemical element carbon acts as a curing agent and having the role of preventing iron atoms, which are naturally arranged in a crystal grid from sliding over each other (displacement). Carbon stock changes and the possible additive elements content (alloy components) will have a strong influence on behavior in solid phase change material. When iron is melted from its ore by commercial processes, it contains more carbon than the desired percentage. To become steel, it must be melted and reprocessed to remove the correct amount of carbon, at which point other elements can be added. High temperature differential scanning calorimetric can provide useful information if these processes were completed to obtain the desired product quality.

It was developed a differential scanning calorimetric test (DSC) in the range temperature RT (room temperature) –1,550 °C with a heating rate of 20 K/min in an argon atmosphere of 50 mL/min for a 173.24 mg sample in a drilling platinum crucible with aluminum insert. Calorimetric analysis result is shown in Fig. 3 and highlights in the left of exothermic transformation direction.

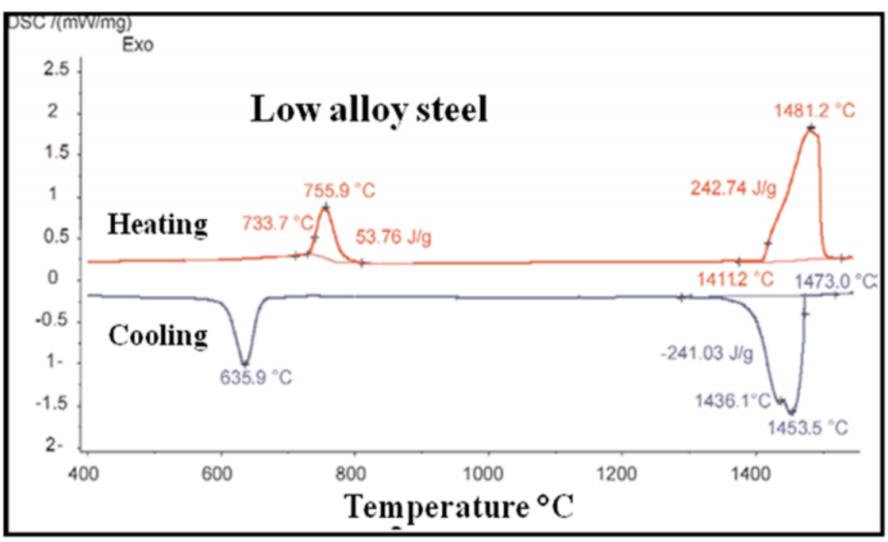

Fig. 3 – The behavior of mild steel in heating calorimetric analysis (DSC).

Shown in Fig. 3 is the chart of specific heat flow measuring of mild steel in the temperature range between 400 and 1,550°C. At 734°C there is a change in crystal structure of the material (from cubic centered volume to the face centered cubic) and can also be observed from energetic point of view. However, it should be noted that in the same temperature range, a change in magnetic properties (from ferromagnetic to paramagnetic) took place. Melting material took place at 1,411°C (solidus temperature). Fusion heat value was 242.7 J/g and liquidus temperature was determined during cooling (the onset of solidification). This was measured at 1,473°C

The solidification heat (–241.0 J / g) is almost the same as the fusion heat. Melting / solidification process double-step character can be seen more clearly during the cooling phase of running. Solid phase transition (solid-solid) that occurs at lower temperatures is also visible during the cooling curve, however, the transformation is shifted to lower temperatures (under cooling).

Inconel alloys are a family of non-magnetic alloys based on nickel. Inconel 600 alloy consists of 72% nickel, 16% chromium and 8% iron. The high content of chromium alloy Inconel 600 raises considerably its resistance to oxidation compared to pure nickel while its high nickel content gives good resistance to corrosion in reduction reaction conditions. Therefore, Inconel 600 material offers high resistance to corrosion and oxidation, even at high temperatures, and also maintain a high mechanical strength under these conditions. It is therefore often used in extreme conditions, such as aircraft engine parts, turbocharger turbine wheels, chemical processing and pressure vessels. Inconel 600 & 800 are also used for pressure tubes of CANDU nuclear reactors. In addition, Inconel 600 is a certified reference material for thermal conductivity.

It was developed a differential scanning calorimetry test (DSC) in the range temperature RT (room temperature) - 1000 °C with a heating rate of 20 K/min in an argon atmosphere of 60 ml/min for a 195.24 mg sample in a platinum crucible drilling aluminum insert. Calorimetric analysis result is shown in Fig. 4.

In Fig. 4 there are presented the six different tests results made on Inconel super-alloys. Differences between individual tests are within ±2%, which corresponds to typical unit accuracy. At lower temperatures, an almost linear increase in specific heat results can be seen. Between 550 and 700 °C, an endothermic step can be observed in the evolution of specific heat. This step can be explained by the formation of clusters Ni3Cr causing an additional contribution to specific heat (Richter and Born, 2004). It should be pointed that the real specific heat is offset by the changes caused by phase transition enthalpy. Therefore, measured data is apparently specific heat in this temperature range.

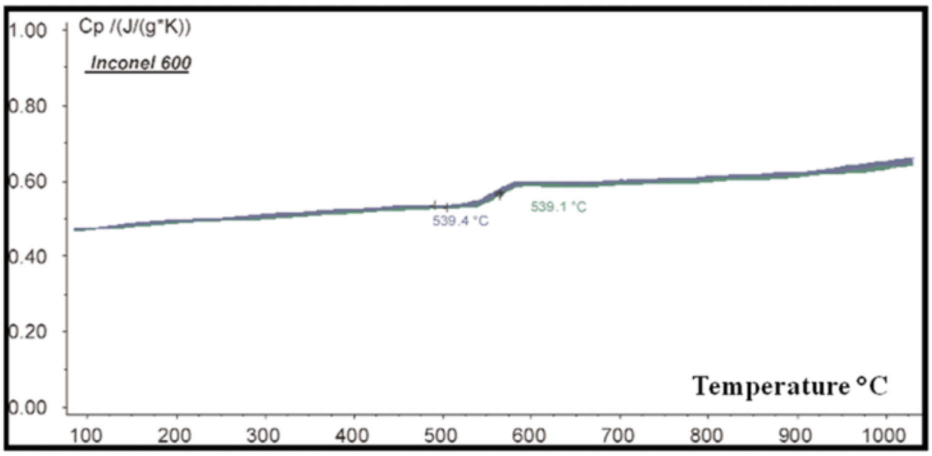

Fig. 4 – The behavior of a nickel-based alloy (Inconel 600) at heating calorimetric analysis (DSC).

Forging is a possible way to shape a metal by plastic deformation. Conventional forging process is performed at high temperatures, making it easier and less likely the appearance of material fractures. Usually, pieces of iron or steel are forged at temperatures at which they become malleable (usually red hot). Cold forging is done at low temperatures. Once the final version was made for iron and steel materials, it is often applied some kind of heat treatment. This can lead to various degrees of materials hardening or softening depending on the technology details to achieve the thermal treatment. Defects during heat treatment in the crystal structure of the material are facing new obtaining temperature resulting a low energy release. This extremely sensitive exothermic effects can be analyzed by differential scanning calorimetric tests Netzsch DSC or STA system.

It was developed a differential scanning calorimetry test (DSC) in the range temperature RT (room temperature) –600°C with a heating rate of 20 K/min in an argon atmosphere of 50 mL/min for a 335.0 mg sample in a drilling platinum crucible with aluminum insert. Calorimetric analysis result is shown in Fig. 5 and highlights exothermic reaction direction.

In Fig. 5 the specific heat flow measured on a cold forged iron sample is shown. During the first heating cycle an exothermic effect was detected at 335°C (extrapolated at the beginning). The peak temperature was at 401°C: at almost 500°C, exothermic reaction was completed. Energy release during the relaxation of this reaction was 0.47 J/g. The effect is not visible analyzing the annealed material. These tests require a high quality vacuum instrument also purging pure gases (to avoid oxidation effects that may occur in a similar temperature range), and also need a high quality of DSC sensor with high sensitivity, reduced background noise and stability. These requirements are standard features of DSC and STA Netzsch systems at high temperatures.

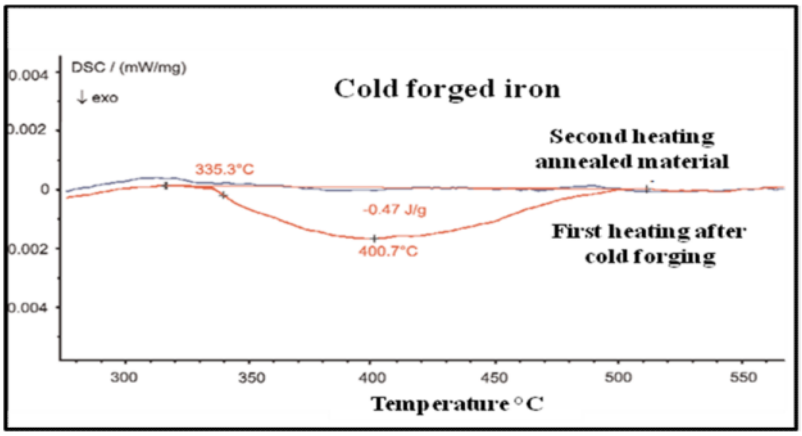

Fig. 5 – A cold forged iron behaviors to a heating calorimetric analysis (DSC).

High performance TiAl alloys are distinguished by their usefulness at high temperatures and corrosion resistance, and a low specific weight. There are used, for example, at turbo chargers, turbines, engines and aircraft and space applications. This could be considered a proper alloy to be investigated with STA (TG + DSC) equipment. Usually the melting phase transformations and mass changes due to oxidation or reduction can be observed.

It was developed a differential scanning calorimetry test (DSC) in the range temperature RT (room temperature) –1,600°C with a heating rate of 20 K/min in an argon atmosphere of 70 mL/min for a 30.08 mg sample in a drilling platinum crucible with aluminum insert. Calorimetric analysis result is shown in Fig. 6 and highlights exothermic reaction direction.

DSC calorimetric signal has an endothermic effect (peak temperature at 1,322°C) beginning at the extrapolation temperature of 1,195°C, this is due to structural $\alpha 2 \rightarrow \alpha$ transformation. At 1,476°C (DSC peak temperature) the $\alpha \rightarrow \beta$ transformation took place.

DSC endothermic peak at 1,528°C is due to the melting process of the sample (beginning at about 1,490°C, and liquidus temperature is recorded at about 1,560°C). There is no significant change in mass that is detected during the experiment indicating that the sample was not oxidized during the experiment.

Titanium alloys are metallic materials that contain a mixture of titanium and other chemical elements. Such alloys have extraordinary properties such as very high tensile strength and toughness (even at extreme temperatures), light weight, corrosion resistance and ability to withstand extreme temperatures.

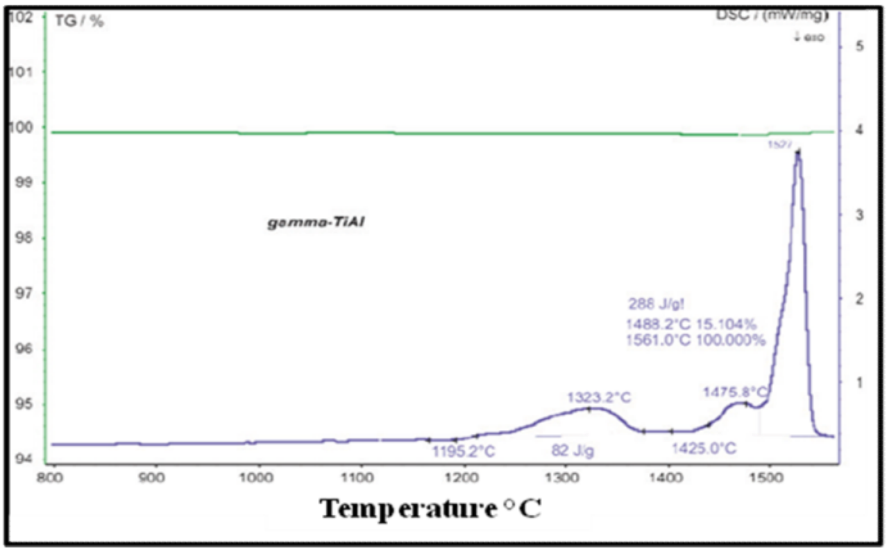

Fig. 6 – Behavior of the TiAl alloy heating calorimetric analysis (DSC).

However, the high cost of raw materials and the difficulty of materials processing limits their use to military applications, aircraft, spacecraft, medical devices, some premium sports equipment and consumer electronics. The addition of chromium to titanium in concentrations above 10% wt helps improve combustion resistance of titanium alloys. For a chromium content greater than 15% chromium alloys have sufficient to withstand an intense combustion environment such as aircraft engines operating at temperatures up to about 510° C. In addition, these alloys could be solidified in the partially amorphous form by rapid cooling process.

It was developed a differential scanning calorimetry test (DSC) in the range temperature RT (room temperature) –1,525°C with a heating rate of 20 K/min in an argon atmosphere of 50 mL/min for a 83.06 mg sample in a drilling platinum crucible. Calorimetric analysis result is shown in Fig. 7 and highlights exothermic reaction direction.

Shown in the graph of Fig. 7 is the apparent specific heat of chromium-titanium alloy at room temperature and 1,525°C range. At 723°C (peak temperature) the specific heat is superimposed by the cold crystallization of amorphous content.

General endothermic effect at approximately 1,211°C (peak temperature) is caused by phase transition from α-phase to *β*-phase. Alloy melting process started at 1,400°C and fusion heat was 282.3 J/g. Even in the liquidus region, there is no overlapping oxidation and therefore no decrease in the measured specific heat was not observed. This can be achieved only if it is used for purging extremely pure gases and special crucibles (yttria covered crucibles).

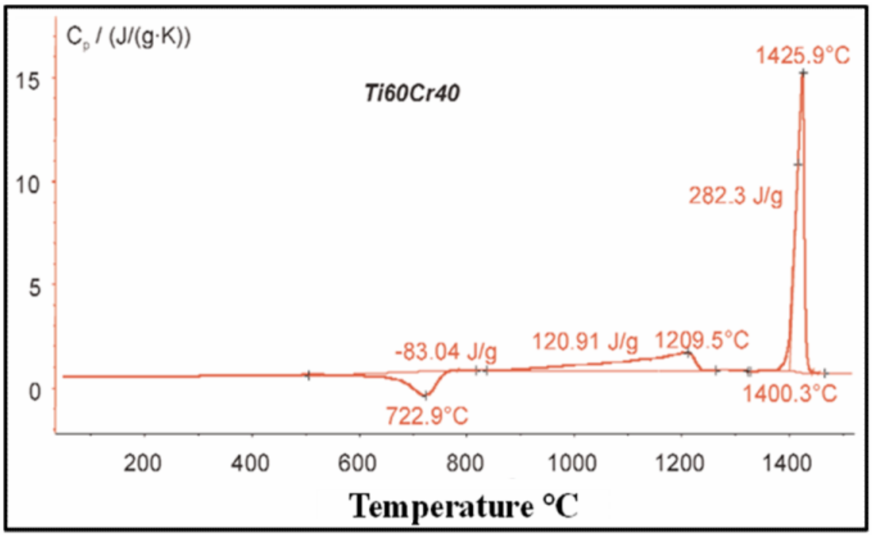

Fig. 7 – The TiCr alloy behavior to a heating calorimetric analysis (DSC).

Zirconium nitride is a refractory ceramic with a high melting point (2,960°C) and high density (7.09 g/cm³). This ceramic material was used recently as an alternative to titanium nitride coated drills. Both coatings should keep the drill sharp and cold, especially during cutting. Stability at high temperatures and nuclear radiation stability make it to be one of the most pursued and examined for nuclear materials. It can, for example, be used as a matrix material in the production of nuclear fuel. One of the advantages is that the material has relatively low capacity to absorb neutron source, that are led in the detachment process. Thermo physical properties must be known for process control applications safety.

It was developed a differential scanning calorimetry test (DSC) in the range temperature TC (room temperature) –1560°C with a heating rate of 20 K/min in an argon atmosphere of 50 mL/min for a 191 mg sample in a drilling platinum crucible. Calorimetric analysis result is shown in Fig. 8.

The results show the heat flow increases from 0.4 J/(gK) at room temperature to 0.55 J/(gK); at 1,500°C there is a slight change of the specific heat wich indicates that Debye temperature is at a low level for these nitride ceramic. At over 900°C it was observed a slight decrease in specific heat. This effect is caused by non-stoichiometric relaxation processes in the material sample. During cooling, from 1,156°C, there is an endothermic peak which overlaps with the specific heat.

This peak is caused by a phase change in zirconium oxide, which occurs inside the sample, similar with contamination.

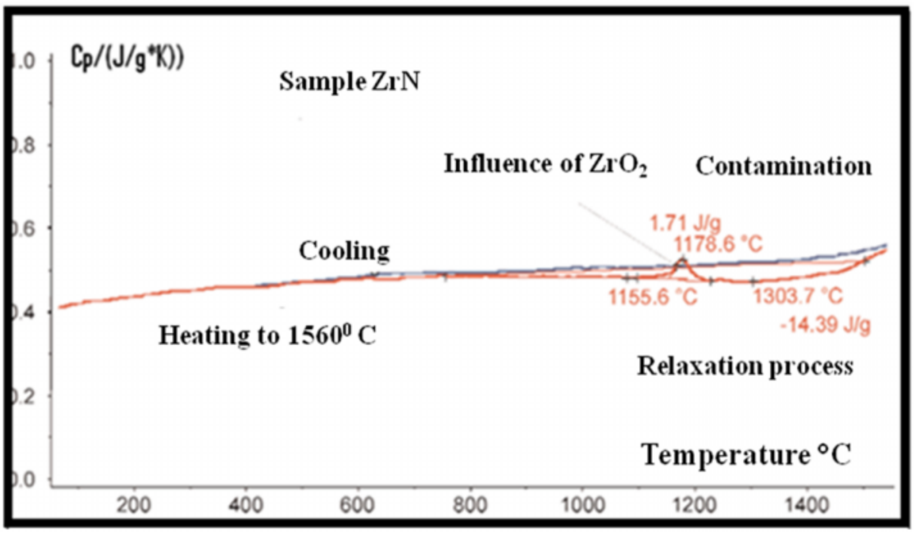

Fig. 8 – The behavior of a ceramic material to heating calorimetric analysis (DSC).

Titanium dioxide (TiO_2) is the most important white pigment. It has valuable properties such as high power coverage, a relatively low price and it is also, chemically inert and also very resistant to light. Wall paint, pharmaceuticals, toothpaste and paper contain, for example, titanium dioxide as a bleaching substance.

There are many sophisticated applications of TiO_2 material: self-cleaning surfaces can be created using photo-catalytic effect of TiO_2 modified. Titanium dioxide, as nanoparticles form, changes color depending on the angle of view that is used in various finishes. Transformation of titanium oxide into rutile at high temperatures may depend strongly by the phases impurity.

It was developed a differential scanning calorimetry test (DSC) in the range temperature TC (room temperature) –1500°C with a heating rate of 10 K/min in an argon atmosphere of 70 mL/min for a 91.34 mg sample in a platinum crucible. Calorimetric analysis result is shown in Fig. 9 and highlights exothermic reaction direction.

STA analysis shows two mass loss steps representing 0.15% and 0.08% below 400°C, which are due most likely to the release of moisture from the sample. At the onset temperature extrapolation of 1,067° C, there was a peak (relatively sharp) with a DSC exothermic transformation enthalpy of –12 J/g indicating the so-called rutilisation operation. At this point anatase modification of TiO_2 turns in rutile.

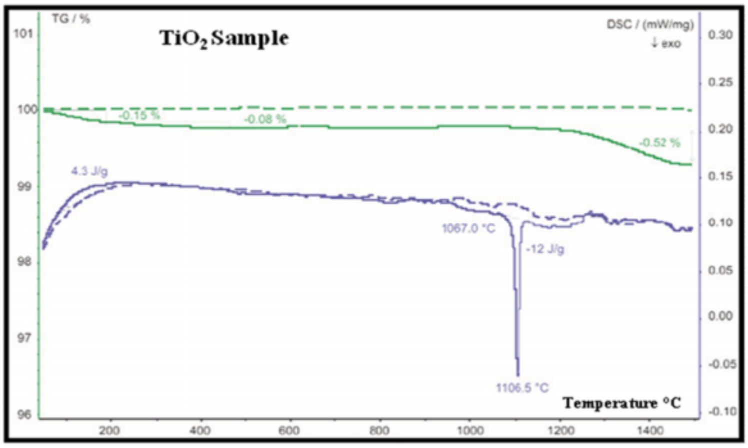

Fig. 9 – Behavior of TiO_2-based material to heating calorimetric analysis (DSC).

At a higher temperature value of about 1,100°C, a 0.52% mass loss was observed that could be caused by the decomposition of sulphates as impurities. The second sample heating (represented by dotted lines) did not show any effects.

Elastomers as natural rubber (CN) / ethylene propylene-diene (EPDM) as rubber are materials with outstanding mechanical properties that can undergo elastic deformation under an external voltage and return to its original size without permanent deformation. Natural rubber (CN) is a polymer composed of several units of isoprene and EPDM is a copolymer of different units of ethylene, propylene and diene.

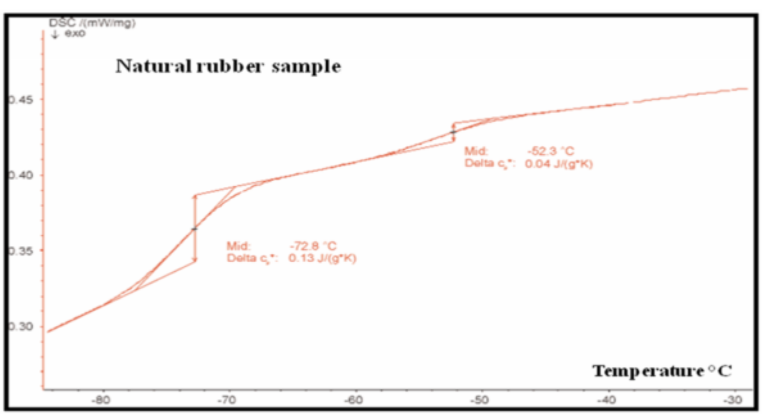

Fig. 10 – The behavior of a polymeric material, natural rubber, to heating calorimetric analysis (DSC).

It was developed a differential scanning calorimetry test (DSC) in the range temperature –100°C and 100°C with a heating rate of 20 K/min in an argon atmosphere of 20 ml/min for a 14.34 mg sample in a drilling aluminum crucible. Calorimetric analysis result is shown in Fig. 10 and highlights exothermic reaction direction.

Two glassy transitions were detected in the evolution of material with temperature changes first at –72.8°C (middle), with changes observed in the specific heat of 0.13 J/(gK), that can be attributed to natural rubber. The second transition has been observed at a temperature of –52.3°C, with a change in the specific heat of 0.04 J/(gK) it is most likely related to glass transition of EPDM component.

Getting materials to ensure efficient storage and safe delivery of hydrogen is considered the major techniques challenge to use hydrogen as an alternative energy carrier. In metal hydrides, the hydrogen element is stable and well secured. This is an advantage in terms of safety requirements for use of alternate materials. Due to a relatively low price and a 7.6% hydrogen content, magnesium hydride (MgH_2) is a promising material for hydrogen storage.

It was developed a differential scanning calorimetry test (DSC) in the range temperature TC and 500°C with a heating rate of 5 K/min in an argon atmosphere for a 2.85 mg sample in a drilling platinum crucible and aluminum oxide. Calorimetric analysis result is shown in Fig. 11 and highlights exothermic reaction direction.

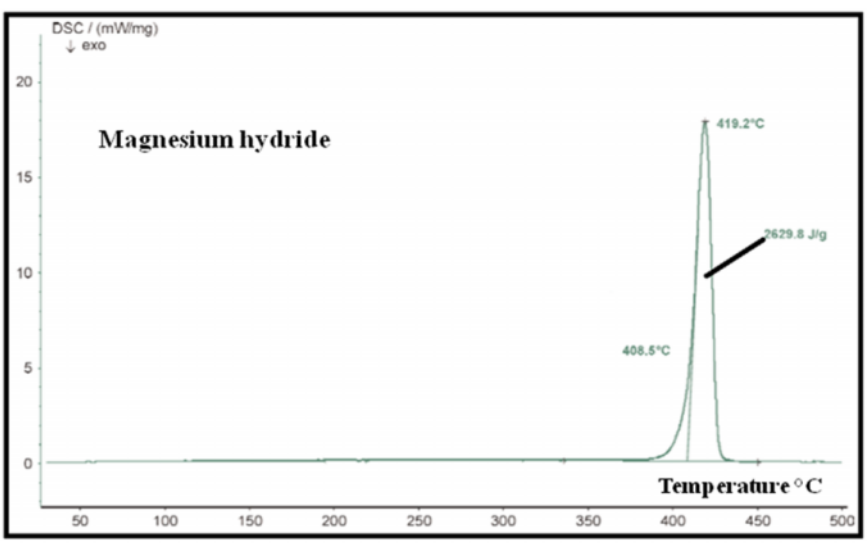

Fig. 11 – The behavior of a material with hydrogen storage properties as MgH_2 to the heating calorimetric analysis (DSC).

DSC investigations of magnesium hydride material indicate that the hydrogen release rate is relatively low up to 300°C. At 408°C temperature (extrapolation of reaction onset), hydrogen is released by a reaction which takes place in one step. A large amount of energy (2,630 J/g) is needed to release hydrogen from MgH_2 material.

Current research activities are conducted to reduce the desorption temperature and to improve sorption speed (absorption). Structural changes are necessary in order to accelerate hydrogen element diffusion in MgH_2. Therefore, several magnesium alloys in combination with another metal are studied regarding their hydrogen absorption behavior.

It is very difficult to achieve a general impression of metal alloys used in dentistry, due to the large amount used today. Several hundred dental alloys are available in the United States, which have been registered with the American Dental Association.

When two or three main components of alloys are known, it is possible to classify them into 4 groups: alloys with a high percentage of gold, alloys with a small percentage of gold, alloys with a percentage of palladium-silver and alloys formed by common metal.

Basic conditions to be fulfilled by a dental alloy for dental applications are its biocompatibility, malleability and resistance to corrosion and even electro-corrosion. Requirement for good biocompatibility of a material is obviously closely linked to resistance to corrosion. Thus, when an alloy is placed in contact with the patient's body, should not cause any harm to the patient health. The purpose of a dental alloy is to be easily manipulated by the dentist but also strong, rigid, durable and resistant to corrosion and loss of gloss. These alloys are used especially for implants, dental crowns and connections.

It was developed a differential scanning calorimetry test (DSC) in the range temperature TC and 1,750°C with a heating rate of 10 K/min in an argon atmosphere of 60 mL/min for a 200 mg sample in a aluminum oxide crucible. Calorimetric analysis result is shown in Fig. 12 and highlights exothermic reaction direction.

Speed heat – flow (DSC) used on dental alloys Pt0.89Au0.1Ir0.01 was recorded up to 1,750°C (three samples were analyzed from the same alloy). Onset melting temperature by extrapolating the trigger was around ~1,659°C. Peak melting occurred at temperatures of about ~1,711°C. Melting enthalpy was ~81 J/g From integral curves of DSC, melting process can be pursued. In general, a good measurements reproducibility can be demonstrated.

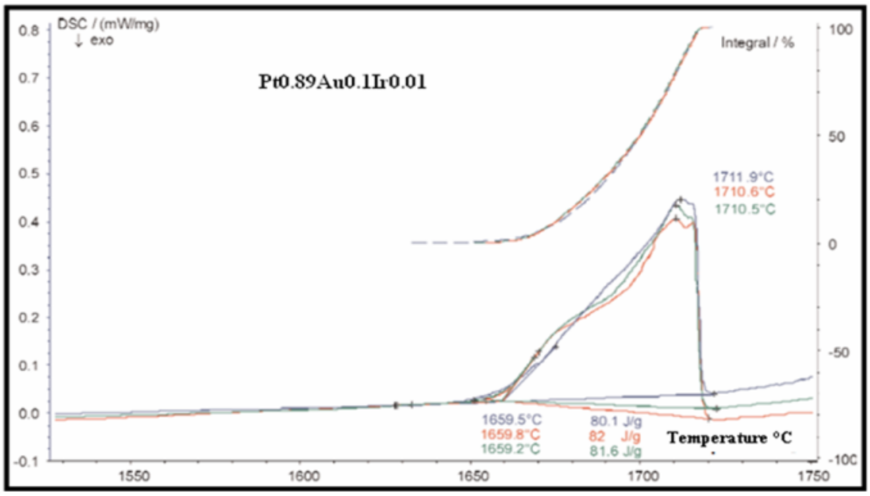

Fig. 12 – The behavior of a dental material to heating calorimetric analysis (DSC).

3. Conclusions

In recent decades this technology has been involved in the study of metallic materials. Low melting materials such as solder are easily examined for example. It is known that it is possible to use DSC to find the solidus and liquidus temperature of a metal alloy, but at this time the widest application is the study of precipitations, and Guiner-Preston zones.

Differential scanning calorimetry represent an impresive tool for materials charcaterisation under thermal effects. Martensitic transformation of a NiTi and a NiTiPd shape memory alloys was charcaterized through DSC on heating and cooling processes. Glass transition on a natural rubber material was observed and the H eliberation from a magnesium hybrid material also was analyzed using differential scanning calorimetry.

REFERENCES

Wunderlich B., *Thermal Analysis*. Academic Press, New York, 137-140, 1990.

Dean J.A., *The Analytical Chemistry Handbook*. McGraw Hill, Inc., New York, 15.1-15.5, 1995.

Pungor E., *A Practical Guide to Instrumental Analysis*. Boca Raton., Florida, 181-191, 1995.

Skoog D.A., Holler F.J., Nieman T., *Principles of Instrumental Analysis* (5 ed.). New York, 805-808, 1998.

O'Neill M.J., *The Analysis of a Temperature-Controlled Scanning Calorimeter*. Anal. Chem. **36,** *7*, 1238-1245 (1964). doi:10.1021/ac60213a020.

* * * U.S. Patent 3,263,484
* * * *DSC Purity Analysis*. http://us.mt.com/mt_ext_files/Editorial/Generic/0/ stare_purity_datasheet_0x000249470002551200005b219_files/ 51724796.pdf. Retrieved 2009-02-05.
* * * *Molecular Biology*. Vol. **6**, Moscow, 1975, 7-33.

REZULTATELE EXPERIMENTALE PRIVIND CALORIMETRIA DIFERENȚIALĂ CU SCANARE LA DIFERITE MATERIALE METALICE ŞI NEMETALICE

(Rezumat)

Tehnica calorimetriei diferențiale cu scanare a fost folosită pentru a analiza comportamentul diferitelor materiale metalice şi nemetalice la variația temperaturii. Douăsprezece material, dintre care: aliajele cu memoria formei, materialele dentare, aliajele special şi superaliajele, ceramic sau materiale hibride cu magneziu au fost investigate prin calorimetrie cu scanare diferențială sub diferite cicluri de încălzire şi răcire iar rezultatele prezentate şi comentate. Au fost utilizate diferite scale de temperatură şi condiții de încălzire DSC pentru a caracteriza câteva materiale şi pentru a începe o bază de date cu rezultate DSC.

BULETINUL INSTITUTULUI POLITEHNIC DIN IAȘI
Publicat de
Universitatea Tehnică „Gheorghe Asachi” din Iaşi
Tomul LVIII (LXII), Fasc. 1, 2012
Secția
ŞTIINȚA ŞI INGINERIA MATERIALELOR

TITANIUM THIN FILMS MOUNTED ON STEELS

BY

ADRIAN ALEXANDRU[*] and GELU BARBU

“Gheorghe Asachi” Technical University of Iaşi
Faculty of Material Science and Engineering

Received: February 28, 2012
Accepted for publication: March 19, 2012

Abstract: The paper presents the experimental results of the authors about the deposition of titanium layers on steels by the electrical discharge method. Titanium layers obtained by this method have-a high corrosion resistance and good mechanical properties. The layer thickness varied between 30…60 µm.

Keywords: electric discharge method, titanium layer deposition, corrosion resistance

1. Introduction

Titanium is one of the most used materials in aero and astronautics, vessels for liquefied gasses, chemical equipment working in corrosive atmosphere ($HN0_3$, HCI, H_2S0_4, etc.), naval engineering (helices, ship frames, submarines, torpilas), cryogenics, nuclear and medical equipments (dental and bone" implants).

The high corrosion resistance of titanium (hundreds of times higher then any stainless steel) is given by the fact that it generates at its surface a very

[*] Corresponding author: *e-mail*: axa72us@yahoo.com

thin film (2 ... 5 nm) of titanium oxide, adherent and compact, which guarantees its passivity.

For permanent protetic works titanium is used with a purity of minimum 99.4% with N < 0.05%, C < 0.06%, O < 0.35% and H < 0.013% from the classes of Ti1, Ti2, Ti3 and Ti4 according to DIN.

Titanium, which has a large number of properties favorable for a broad area of applications, is an adverse metal and consequently, very expensive. A join of the many titanium favorable properties with an acceptable cost, especially in the medical field, is possible only by using thin films of titanium produced through various methods: electric spark, vapors chemical mounting, ionic implant, electric spark with vibrating electrode, etc.

The electric spark mounting is the most efficient and simple method, since one can get layers of 0.01 ... 0.03 mm, very adherent to the base material; the link layer-base material is achieved through a diffusion sublayer which ensures a perfect cohesion.

When the metallic electrode (anode) is approached or removed from the processed material (cathode), for a very short period of time, an electric spark is produced, which develops a temperature of about 15,000°C vaporizing the anode and cathode materials, and producing between the electrodes a dense plasma of ions and atoms.

The quench (about 10^5 °C/s) of the mounted white layer leads to an alteration of its structure into a nanocrystalline one (even amorphous) with remarkable properties concerning hardness, wear resistance, corrosion resistance or even biocompatibility.

2. Research Technique

In order to achieve titanium thin films one picks an electric spark method given by a titanium electrode (0.11% O, 0.01% N, 0.01% C, 0.06% Fe, 0.001% H and 99.8% Ti), with 3.0 mm in diameter. We used an ELITRON 22 type installation with a discharge current of 1.5 A for the first layer, and of 0.8 A for the second layer. The second layer was mounted using a weaker regime in order to improve rugosity.

The analysis was accomplished on three marks of Romanian steels in delivery state, with compositions given in Table 1.

Table 1

Steel	C, [%]	Mn, [%]	Si, [%]	Cr, [%]	Ni, [%]	Mo, [%]
OLT35	0.1	0.6	0.3	–	–	–
14MoCr10	0.1	0.4	0.15	0.9	–	0.5
2MoNiCr175	0.1	0.1	0.1	18.2	14.5	2.6

Paralellipipedic (15 × 10 × 5 mm), rectified steel samples, with titanium layers mounted by electric spark, were analyzed for the thickness of the mounted and diffused layer, rugosity, microhardness, optical metallographic, diffractographic phase, and now they are subjected to biocompatible tests, a long term analysis.

3. Experimental Results

3.1. Mechanical and Geometrical Characteristics

These characteristics were determined in the cross section of the layer mounted on preliminary polished, cleaned and chemically treated (specific to each type of steel) samples.

Table 2*

Sample	MHV_{20}			Thickness, [µm]		R_a µm
	Base layer	Diffusion layer	Mounted layer	Diffusion layer	Mounted layer	
Ti	288.6	–	–	–	–	–
OLT35	200.1	299.7	802.5	12	35	1.2
14MoCr10	328.7	401.7	674.3	10	28	1.2
2MoNiCr175	220.2	379.3	574.2	12	31	1.2

*Obs. All of the above values are the result of an average over three measurements.

Results of Vickers microhardness for a load of 0.02 kg, thickness of the mounted and of the diffusion layer and rugosity measurements are given in Table 2 (Alexandru *et al*., 1997).

The traces left by the diamond top are visible in the microstructures showed in Figs. 1,…,3. One can find that titanium microhardness increased from about 288.6 daN/mm^2 in the delivery state up to 574 ... 802.5 daN/mm^2 in the mounted layers. This substantial microhardness increment may be explained by a microstructural change (extreme structure refinement), an increase of the stress state or by the change of the chemical composition of the mounted layer by diffusion of some of the elements from the base material, this later fact still remaining to be proved by electron microscopy, electron and X rays diffraction (TEM and EDAX).

In general, the micro-hardness of the diffusion layer situates between the value for the mounted layer and that for the base material.

The thickness of the deposited (white) layer and of the diffusion layer of 28...35 Htn and 10...12 µm, respectively, correspond to the working regimes. Rugosity of the mounted layer surface, R_a = 1.2 urn reflects the intensity of the discharging regime used in the second deposition. It is bigger the higher is the discharging regime (Deac, 1992).

3.2. Microstructural Analysis

The microstructural analysis was performed with a 300:1 grosissment microscope in perpendicular sections of the titan mounted layer.

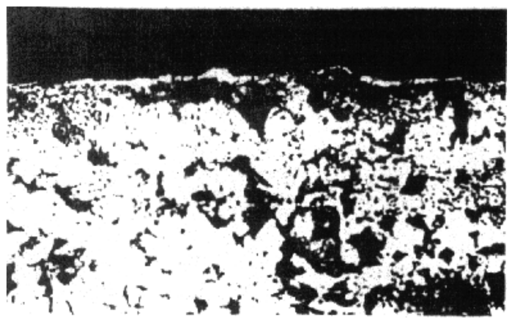

a

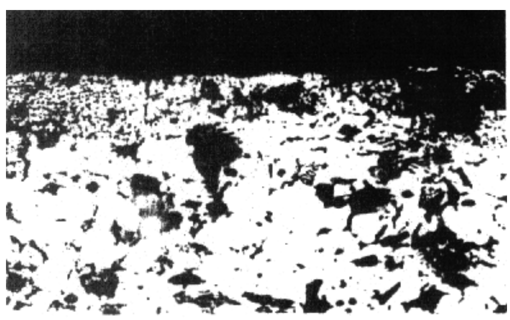

b

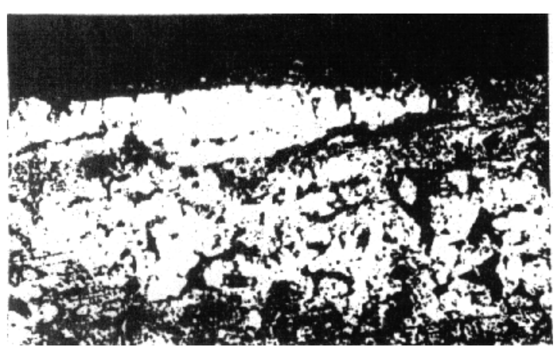

c

Fig. 1 – OLT 45 steel coated with Ti by electric spark. Attack: nitol 3%, 300:1.

Measurements of the base material, deposited titanium (white) layer and diffusion of the steel OLT35, in different areas are highlighted in Figs. 1 *a*, *b*, *c*.

The base material is made Of ferrite and perlite. The mounted layer has a nonuniform thickness, and the diffusion layer is very narrow. The alloyed steel 14MoCr10 covered with titanium by electric spark has the structure given in Figs. 2 *a*, *b*, *c*. One observes that, basically, the structure consists of a ferrite matrix with primary (white, big) segregated and secondary (small, white) uniformly distributed carbides. The mounted titanium (white) layer is well emphasized and has a nonuniform thickness, but the diffusion sublayer is very thick.

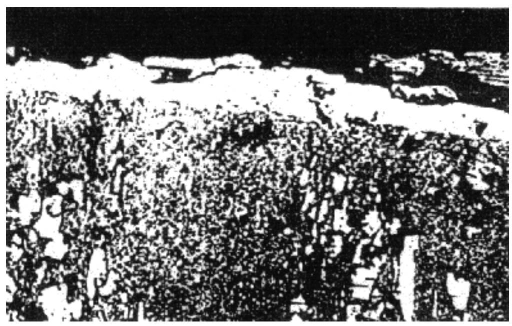

a

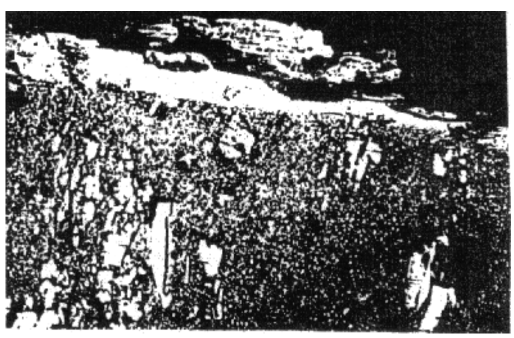

b

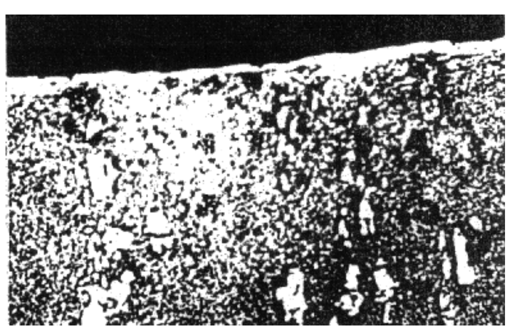

c

Fig. 2 – 16MoCr10 steel coated with Ti by electric spark. Attack : nitol 3%, 300:1.

The stainless steel 2MoNiCc175 coated with titanium, shows microstructures depicted in Figs. 3 *a* and *b*. In this case, the titanium layer is hardly visible since the chemical.

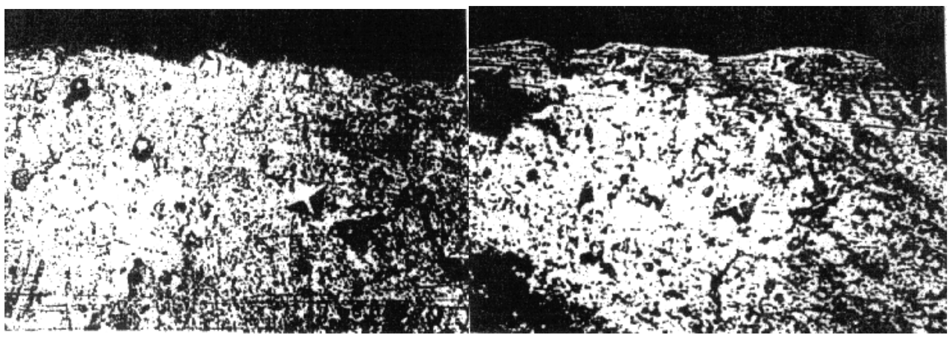

a *b*

Fig. 3 – 2MoNiCr175 stainless steel coated with Ti by electric spark. Attack: 1/3 HCI, 2/3 H_2S0_4; 300:1.

Reactive used for the stainless steel attacked the external white layer too. The external white layer presence is emphasized by the tracks left by the diamond top microhardness apparatus. The base material in this case is austenitic (Morton & Bell, 1990).

The microstructure of the titanium electrode used for coating is typically for casting and has a dendritic peculiarity as shown in Fig. 4.

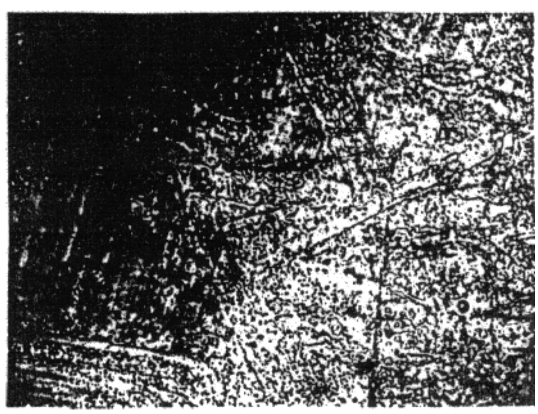

Fig. 4 – Titanium electrode microstructure.

4. Conclusions

1. Titanium – metal with unusual features can be easily mounted in thin films on steel surfaces.

2. The electric spark deposited titanium layer has a hardness which is 2...3 times higher than in its normal state, and adheres to the base steel through a diffusion layer.

3. The unusual properties of the layer are ensured both by phase structural changes, and by its stressed state.

4. Further specific tests concerning corrosion are necessary in order to finish the researches.

REFERENCES

Alexandru I., Burlui V., Alexandru A., *Straturi subţiri de materiale şi biomateriale metalice depuse prin scânteie electrică*. Sesiunea Ştiinţifică „Sf. Apollonia", Iaşi, 1997.

Deac V., *Titanul ca material de restaurare protetică*. Conferinţa de tratamente termice şi termochimice, Cluj-Napoca, 1992.

Morton P.H., Bell T., *Les proceeds technologique des surface appliqués au titan*. Treatment Thermique, *241*, Paris (1990).

FILME SUBŢIRI DE TITAN DEPUSE PE OŢELURI

(Rezumat)

Se prezintă rezultatele experimentale ale autorilor cu privire la depunerea de straturi de titan pe oteluri prin metoda descarcarii electrice. Straturile de titan obţinute prin această metodă au o rezistenţă ridicată la coroziune şi proprietăţi mecanice bune. Grosimea stratului a variat între 30...60 μm.